ELECTRONIC TRANSPORT IN A BOUNDARY-DRIVEN ONE-DIMENSIONAL CHAIN WITH BULK DEPHASING

A Thesis Submitted to
the Graduate School of
İzmir Institute of Technology
in Partial Fulfillment of the Requirements for the Degree of

MASTER OF SCIENCE

in Physics

by
Hakan YELER

July 2024

İZMİR

We approve the thesis of **Hakan YELER**

Examining Committee Members:

Assoc. Prof. Dr. Özgür ÇAKIR
Department of Physics, IZTECH

Prof. Dr. Alev Devrim GÜÇLÜ
Department of Physics, IZTECH

Prof. Dr. Ahmet Levent SUBAŞI
Department of Physics Engineering, ITU

12 / July / 2024

Assoc. Prof. Dr. Özgür ÇAKIR
Supervisor, Department of Physics
IZTECH

Prof. Dr. Lütfi ÖZYÜZER
Head of the Department of
Physics

Prof. Dr. Mehtap EANES
Dean of the Graduate School

ACKNOWLEDGMENTS

I want to express my sincere thanks to my supervisor Dr. Özgür Çakır who has shaped my understanding of physics since my undergraduate years, for our insightful conversations during my research process. I am also grateful to both Prof. Alev Devrim Güçlü and Prof. Ahmet Levent Subaşı from my thesis committee for their valuable feedbacks which improved the quality of my work. Finally, I would like to express my gratitude to my family and my friends for their support and making this process fun.

ABSTRACT

ELECTRONIC TRANSPORT IN A BOUNDARY-DRIVEN
ONE-DIMENSIONAL CHAIN WITH BULK DEPHASING

This thesis investigates the non-equilibrium steady state transport properties of interacting and non-interacting fermions on 1D chain under environmental effects with the help of the Lindblad master equation. The current operator which is used for the characterization of the transport is defined. Because many-body systems pose computational challenges due to their exponentially growing Hilbert space, different solution methods are studied. The covariance matrix method is introduced for the non-interacting case, because of the computational advantage. Approximate methods like the mean-field and the hierarchy of correlation functions are introduced and compared among themselves for the interacting case. Behavior of the transport is studied via exact solution method. Vectorizing the Lindblad master equation, a system of linear equation is obtained. Using Python programming language and solving the system of the linear equation, the non-equilibrium steady state density matrix and the current as a function of environmental variables are calculated.

ÖZET

SINIRDAN GÜDÜLEN BİR BOYUTLU ZİNCİRDE
YIĞIN EŞEVRE KAYBI ALTINDA ELEKTRONİK TAŞINIM

Bu tezde, etkileşimli ve etkilemşimsiz fermiyonların bir boyutlu zincir üzerinde denge dışı durağan durumdaki taşınım özellikleri, çevre etkilerini de hesaba katarak incelenmiştir. Sistem dinamiği Lindblad master denklemi kullanılarak hesaplanmıştır. Taşınımı karakterize eden akım operatörü tanımlanmıştır. Hilbert uzayının eksponansiyel artış göstermesi sebebiyle, çok parçacıklı sistemlerin çözümünü hesaplamak zordur. Bu sebeple farklı çözüm metodları incelenmiştir. Hesaplama avantajlarından dolayı, etkileşimsiz sistemlerin çözümü için kovaryans matris methodu tanıtılmıştır. Etkileşimli sistemler için ortalama alan ve korelasyon fonksiyonların hiyerarşisi gibi yaklaşık metodlar tanıtılıp, birbirleriyle kıyaslanmıştır. Taşınımın davranışı kesin çözüm yöntemi yardımıyla incelenmiştir. Lindblad denklemi vektörize edilerek doğrusal denklem sistemi elde edilmiştir. Elde edilen doğrusal denklem sistemi, Python programlama dili kullanılarak çözülmüştür. Denge dışı durağan durum yoğunluk matrisi ve akım, farklı çevre parametrelerine göre hesaplanmıştır.

TABLE OF CONTENTS

LIST OF FIGURES

LIST OF TABLES

Table **Page**

CHAPTER 1

INTRODUCTION

The transport phenomenon has been a subject of research for many years. With our increasing knowledge in the field of quantum and developing technology, the direction of research has shifted from macroscopic to microscopic transport. Potentially substantial advances in nanotechnologies could arise from improvements in our knowledge of transport at the quantum scale. Non-unitary dynamics of transport is an important research topic because of real-world applications. Today, in a wide range of systems, from biological systems to optical fiber cavity networks,[1–9] enhancement of transport efficiency due to system-environment interactions is well understood. It has been shown that particles that are localized due to disorder in the system transition to delocalized states due to dephasing. This phenomenon is called environment-assisted quantum transport (ENAQT).[10] Also, many-body open quantum systems have a wide literature, both numerically and experimentally, in both fermionic and bosonic systems, organic and artificial systems.[11–16] For more detailed information, theoretical[17] and experimental[18] review articles can be helpful. But there are still unknowns waiting to be discovered.

One of the most important reasons that paved the way for studies in this new field is the development of open quantum system theory. Due to the non-negligible effects of the environment, a new framework has been created in which energy and information exchange with the environment is included, instead of the framework laid by Schrödinger, Heisenberg, and Dirac. For open quantum dynamics, there are various formalisms. One of them is the Lindblad formalism.[19] With several approximations, environments' degrees of freedom can be ignored, and effective master equation is used.[20] Although it is common to derive the Lindblad master equation from microscopic models, the equation will be different for each bath and system Hamiltonian and the jump operators will not be local. Therefore, to capture the main physics of transport and its relation to dephasing and particle-particle interaction, we preferred to use the phenomenological model. It was also shown that local coupling of reservoir is a good approximation to more realistic models.[21]

Transport occurs as a result of the interaction of the reservoir with the environment at different temperatures or potentials, and when sufficient time passes, the system tends to enter a non-equilibrium steady state (NESS). During the work, instead of the dynamics of the system, steady-state properties of the system are investigated. In addition to the ease of calculation, the fact that many natural systems operate in steady state is a good reason

for this choice.[9] This thesis is organized as follows:

- In Chapter 2, the general framework of the open quantum system is explained and basic examples of non-unitary processes are shown. The quantum Zeno effect which also seen in this study is presented.

- In Chapter 3, the Hamiltonian and the Lindblad operators used throughout this thesis are presented. The particle current operator is defined.

- In Chapter 4, different methods used to solve dynamics of the system is presented. Approximate methods like the mean-field and the hierarchy of correlation functions are introduced. Their pros and cons are studied. Exact solution method is introduced. The results of this thesis are presented. The concept of transport regime is introduced and its change with dephasing is demonstrated. In the strongly correlated systems, the change of the Zeno regime and the local maximums occurring in the current because of driving rate Γ are shown. Also, dephasing enhanced transport and its mechanism are explained.

CHAPTER 2

OPEN QUANTUM SYSTEMS

As in everything else, nature does not care about our idealizations and tries to interact with our systems as much as it can. For this reason, the concept of "closed system" appears only in textbooks or as a first step we use in understanding the nature of things. Therefore, instead of the framework put forward by Schrödinger, Heisenberg and Dirac, a new framework was created that included the exchange of energy and information with the environment. In this chapter, I briefly explain the formalism that I used throughout this work and the general framework that describes the evolution of open systems. Also, a basic open quantum system example and the Zeno effect are presented. The Zeno effect is a feature of quantum-mechanical systems.

2.1 General Framework

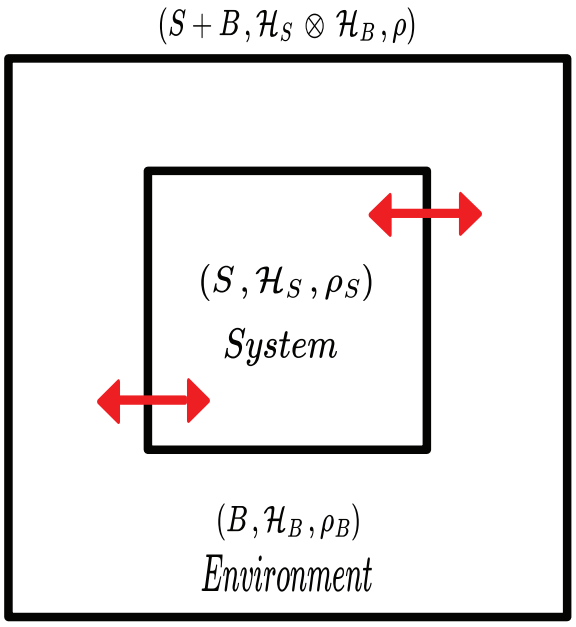

Figure 2.1: Schematic picture of an open quantum system.

As shown in Figure 2.1, an open quantum system is a system S which is coupled to another system B called environment or bath. System S and B can exchange particles, energy or information between themselves. In general, combined system S + B is assumed closed system. Therefore, dynamics of combined system S + B is governed by Schrödinger equation. The total Hamiltonian, defined as

$$H = H_S \otimes I_B + I_S \otimes H_B + H_I \tag{2.1}$$

where H_S and H_B are the self Hamiltonian of the open system S and the environment B respectively, H_I is the Hamiltonian describing the interaction between the system and environment and $I_{\{\bullet\}}$ is the Identity operator for the Hilbert space $\{\bullet\}$. The most general form of the interaction Hamiltonian H_I is,

$$H_I = \sum_{\alpha} A_\alpha \otimes B_\alpha \tag{2.2}$$

where operators A_α and B_α are only act on the open system S and environment B, respectively. Because degrees of freedom of environment is enormous, using direct calculation for dynamics is basically impossible. Luckily, any observation of interest refer only to the open system S and their expectation values are calculated as,

$$\langle \mathcal{O} \rangle_t = Tr\{\mathcal{O}\rho_S(t)\} \tag{2.3}$$

where

$$\rho_S(t) = Tr_B\{\rho(t)\} \tag{2.4}$$

is the reduced density matrix[20] of the system S obtained by tracing out all degrees of freedom of the environment B. $Tr_{\{\bullet\}}$ denotes the partial trace over the subsystem $\{\bullet\}$.

The equation governing time evolution of the reduced density matrix of the system S should be in the following form,

$$\frac{d}{dt}\rho_S = -i[H_S, \rho_S] + \Delta\tilde{\rho_S} \tag{2.5}$$

where the first term on the right side represents the unitary part of the dynamics generated by the Hamiltonian H_S and the second term represents required correction because of system environment coupling. The main goal of all different open quantum systems approaches is to find the correction term $\Delta\tilde{\rho}_S$. The most general and formally exact approach to this correction term is

$$\Delta\tilde{\rho_S} = \int_{-\infty}^{t} dt' F(t-t')[\rho_S(t')] \tag{2.6}$$

called Nakajima-Zwanzig equation[22] where F is a functional of the reduced density matrix $\rho_S(t')$. The differential equation in Equation (2.6) is not only depends on current state of the system, also past states of the system. First approximation will be ignoring this memory effect and making the process Markovian. In Markovian regime Equation (2.5) will be in this form,

$$\frac{d}{dt}\rho_S = -i[H_S, \rho_S] + F[\rho_S(t)] \tag{2.7}$$

the condition underlying this approximation is that system-reservoir interaction rate is much smaller than escape rate of excitations in reservoir. In other words, bath correlation functions decay fast with respect to relaxation time of the system.

The form of the second part of the Equation (2.7) can be determined exactly or with different approximations from microscopic models. One of them is Redfield equation, which is approximation to Nakajima-Zwanzig equation up to second order correction. However, it does not guarantee protecting positivity of density matrix. Also, there is an approach which does not take into account microscopic form of system and bath and preserve positivity. It is called Lindblad master equation and used during this work.

2.2 Lindblad Master Equation

Lindblad formalism emerged from the question "What should a Markovian equation of motion look like?". It is a general form of the Markovian master equation. It can also be derived from microscopic models like Redfield equation. If the level spacing of system energy levels is much larger than the level broadening arising from environment interactions, a secular approximation can be applied to the Redfield equation and the Lindblad form is obtained. A basic requirement that Lindblad form should provide is mapping any density matrix to another density matrix. In other words, it preserves Hermiticity, trace and positivity of density matrix. The Lindblad master equation for system's density matrix ρ can be written as[20]

$$\frac{d}{dt}\rho = -\frac{i}{\hbar}[H,\rho] + \sum_k \gamma_k \left(L_k \rho L_k^\dagger - \frac{1}{2}\left\{ L_k^\dagger L_k, \rho \right\} \right) \tag{2.8}$$

where $\{,\}$ is anticommutator, ρ is system density matrix, hereafter I will ignore S subscript from system related terms, H is the system Hamiltonian, describing unitary part of the dynamics, and L_k are set of jump operators, describing non-unitary part of the dynamics. For simple physical insight, Equation (2.8) can be thought as during time dt system evolve with effective Hamiltonian

$$H_{eff} = H - \frac{i\hbar\gamma_k}{2} L_k^\dagger L_k \tag{2.9}$$

then with probability $\gamma_k \langle L_k^\dagger L_k \rangle$dt jump to new state

$$\rho \rightarrow \frac{L_k \rho L_k^\dagger}{Tr(L_k^\dagger L_k \rho)} \tag{2.10}$$

2.3 Single Qubit Coupled To A Bath

To better understand the Lindblad master equation and different bath effects, let us introduce an illustrative example. In this example, $\hbar$ is set equal to 1. A single spin system with the Hamiltonian

$$H = \frac{\Omega}{2}\sigma_z \tag{2.11}$$

coupled to a spin bath with inverse temperature $\beta = 1/k_B T$. The bath considered as infinite number of independent spin with the Hamiltonian

$$H_B = \sum_j \frac{\omega_j}{2}\sigma_z. \tag{2.12}$$

A basic Lindblad master equation causing the diagonal elements of the density matrix to change is

$$\frac{d}{dt}\rho = -i[H,\rho] + \Gamma(1-f)\mathcal{D}[\sigma^-](\rho) + \Gamma f \mathcal{D}[\sigma^+](\rho) \tag{2.13}$$

where $\mathcal{D}[L](\rho) = L\rho L^\dagger - \frac{1}{2}\{L^\dagger L, \rho\}$, Γ is coupling strength, and $0 \leqslant f \leqslant 1$ which represent bias between rising and lowering is the Fermi-Dirac distribution

$$f = \frac{1}{e^{\beta\Omega}+1}. \tag{2.14}$$

This can be understood considering single spin system coupled to the bath with the interaction Hamiltonian $H_{int} = \sum_j g_j(\sigma^- b_j^\dagger + \sigma^+ b_j)$ where b_j and $b_j^\dagger$ are lowering and rising operator respectively for the j^{th} spin in spin bath. Each spin has ω_j level spacing. Like the Fermi-Golden rule, when the system level spacing Ω equals bath spins' level spacing ω_j, the system and the bath interaction will resonate. Then the rising rate will be

proportional to the Fermi-Dirac occupation number f($\omega_j = \Omega$).

The density matrix of the system is parametrized as

$$\rho = \begin{pmatrix} \rho_{ee} & \rho_{eg} \\ \rho_{ge} & \rho_{gg} \end{pmatrix} \tag{2.15}$$

where ρ_{ee} and ρ_{gg} are excited and ground state population, respectively. Using Equation (2.13), time evolution of the density matrix

$$\rho(t) = \begin{pmatrix} (\rho_{ee}(0) - f)e^{-\Gamma t} + f & e^{-i\Omega t}\rho_{eg}(0)e^{-\Gamma t/2} \\ e^{i\Omega t}\rho_{ge}(0)e^{-\Gamma t/2} & (f - \rho_{ee}(0))e^{-\Gamma t} + 1 - f \end{pmatrix} \tag{2.16}$$

is obtained. It is seen that non-unitary dynamics changes population terms and also affects the coherence in Equation (2.16). The system will relax to the thermal state,

$$\rho_{th} = \frac{e^{-\beta H}}{Z} = \begin{pmatrix} f & 0 \\ 0 & 1 - f \end{pmatrix}. \tag{2.17}$$

Another type of bath is the dephasing bath. It does not change the population of the states, only changes the coherence. The Lindblad master equation representing dephasing and unitary evolution is

$$\frac{d}{dt}\rho = -i[H, \rho] + \gamma \mathcal{D}[\sigma_z](\rho) \tag{2.18}$$

An analytic expression of the density matrix obtained as

$$\rho(t) = \begin{pmatrix} \rho_{ee}(0) & \rho_{eg}(0)e^{-i\Omega t}e^{-\gamma t} \\ \rho_{ge}(0)e^{i\Omega t}e^{-\gamma t} & \rho_{gg}(0) \end{pmatrix} \tag{2.19}$$

The coherence decays with time. It can be thought of as a Bloch vector making a helical move while the length of the vector is shrinking.

2.4 The Quantum Zeno Effect

One of the most fascinating results of quantum mechanics is the quantum Zeno effect. While the measurement frequency increases, the dynamics of the system slows down. In order to demonstrate quantum Zeno effect[23] for ideal and continuous measurement, consider observable A that has discrete and non-degenerate eigenvalues. Operator A can be expressed as;

$$A = \sum_n \lambda_n \left|\Phi_n\right\rangle\left\langle\Phi_n\right| \tag{2.20}$$

where $\left|\Phi_n\right\rangle$ and λ_n are eigenstates of operator A and corresponding eigenvalues, respectively. Assuming that the system initially prepared as eigenstate

$$\left|\Phi(0)\right\rangle = \left|\Phi_k\right\rangle. \tag{2.21}$$

With the help of Taylor expansion of the Schrödinger equation

$$\left|\Phi(t)\right\rangle = [I - iHt - \frac{1}{2}H^2t^2 + ...]\left|\Phi(0)\right\rangle \tag{2.22}$$

probability of obtaining λ_k after measurement at t = θ, is calculated as

$$P_k(\theta) = \left|\left\langle\Phi_k|\Phi(\theta)\right\rangle\right|^2 = 1 - (\Delta E)_k^2\theta^2 + \mathcal{O}(\theta^4) \tag{2.23}$$

$$(\Delta E)_k^2 = \langle \Phi_k | H^2 | \Phi_k \rangle - \langle \Phi_k | H | \Phi_k \rangle^2 \tag{2.24}$$

If measurements are made at θ intervals, probability of getting λ_k after time $\tau = N\theta$

$$P_k(\tau) \approx [1 - (\Delta E)_k^2 \theta^2]^N \tag{2.25}$$

At continuous measurement limit $\theta = \frac{\tau}{N} \longrightarrow 0$ leads to N $\longrightarrow \infty$ for fixed τ

$$P_k(\tau) \approx \left[1 - (\Delta E)_k^2 \frac{\tau\theta}{N}\right]^N \approx exp[-(\Delta E)_k^2 \tau\theta] \longrightarrow 1 \tag{2.26}$$

It means that system will not evolve, stay at initial state. Like ideal measurement, non-ideal measurement also causes the quantum Zeno effect. The Lindblad jump operators can be thought as measurement operators and The Lindblad dynamics can be considered as an indirect continuous monitoring of the system.

CHAPTER 3

BOUNDARY-DRIVEN QUANTUM CHAINS

In this chapter, I described the boundary-driven fermionic chain model. It is the model which is used during this thesis to study transport properties in open quantum system. In the first section, the system Hamiltonian is introduced. In the second section, the environment is introduced. In the last section, current, which is used for characterization of transport, is presented.

3.1 Fermi Hubbard Model

In order to investigate transport properties, the best way is to start from basic models. The one that is simple and grasping physics of various materials is the Fermi-Hubbard model. It is a good approximation for particles in 1D chain at sufficiently low temperatures. A simple Hamiltonian in second quantized form with field operators $\psi_\sigma(\mathbf{r})$ is the following,

$$\begin{aligned} H = &\sum_{\sigma} \int d^3 r \psi_\sigma^\dagger(\mathbf{r}) \left[-\frac{\hbar^2}{2m} \nabla^2 + U_{ion}(\mathbf{r}) \right] \psi_\sigma(\mathbf{r}) \\ &+ \frac{1}{2} \sum_{\sigma,\sigma'} \int d^3 r \int d^3 r' \psi_\sigma^\dagger(\mathbf{r}) \psi_{\sigma'}^\dagger(\mathbf{r'}) V_{ee}(\mathbf{r} - \mathbf{r'}) \psi_{\sigma'}(\mathbf{r'}) \psi_\sigma(\mathbf{r}) \end{aligned} \tag{3.1}$$

which represents the kinetic energy, lattice potential with periodicity given by lattice vector $\mathbf{R}_i$ and Coulomb interaction, respectively. Lattice potential obtained by the Born-Oppenheimer approximation. Because nuclei are much heavier than the electrons, nuclei are thought of as fixed in space. Dynamical lattice effects are neglected.

The first idea that comes to mind when periodicity is seen is the Bloch functions. However, they are delocalized functions in real space. In order to derive the Hubbard model, which is a tight-binding model, more localized functions are needed. In these

cases, Wannier functions that are Fourier transforms of the Bloch states come into play. Wannier functions, defined as

$$\phi_{i\alpha}(\mathbf{r}) \equiv \phi_{\alpha}(\mathbf{r}\text{-}\mathbf{R}_i) = \frac{1}{\sqrt{N}} \sum_{\mathbf{k}} e^{-i\mathbf{k}\cdot\mathbf{R}_i} u_{\mathbf{k},\alpha}(\mathbf{r}) \tag{3.2}$$

where $u_{\mathbf{k},\alpha}(\mathbf{r})$ is Bloch function and α is band index. Wannier functions are localized at the site $\mathbf{R}_i$ of the lattice. Before starting derivation, it is assumed that all the electrons are in the lowest band and other bands are energetically unavailable. At sufficiently low temperature, it is a good approximation. Therefore, there is no need for band index α anymore.

Using Wannier states, creation operators for electrons are defined as

$$b_{i\sigma}^{\dagger} = \int d^3 r \phi_i(\mathbf{r}) \psi_{\sigma}^{\dagger}(\mathbf{r}) \tag{3.3}$$

which have the inverse relation

$$\psi_{\sigma}^{\dagger}(\mathbf{r}) = \sum_i \phi_i^*(\mathbf{r}) b_{i\sigma}^{\dagger} \tag{3.4}$$

Putting Equation (3.4) into Equation (3.1) generalized Hubbard Hamiltonian

$$H = \sum_{ij} \sum_{\sigma} t_{ij} b_{i\sigma}^{\dagger} b_{j\sigma} + \frac{1}{2} \sum_{ijkl} \sum_{\sigma\sigma'} v_{ijkl} b_{b\sigma}^{\dagger} b_{j\sigma'}^{\dagger} b_{k\sigma'} b_{l\sigma} \tag{3.5}$$

is obtained. Considering a lattice of widely spaced atoms, the matrix elements of Equation (3.5) decay fast with increasing distance $|\mathbf{R}_i - \mathbf{R}_j|$ and only nearest-neighbor terms remain. First term in Equation (3.5) describe tunneling of electrons between different sites. The second term is the interaction term that includes Hubbard repulsion, Coulomb

interaction between electrons, bond-charge interaction, Heisenberg exchange interaction, and tunneling of electron pairs. Following Hubbard,[24] all the terms are neglected except hopping and on-site Coulomb interaction terms. The Fermi-Hubbard Hamiltonian

$$H = -t \sum_{i}^{N-1} \sum_{\sigma} \left(b_{i\sigma}^{\dagger} b_{i+1,\sigma} + b_{i+1,\sigma}^{\dagger} b_{i\sigma} \right) + U \sum_{i}^{N} n_{i\uparrow} n_{i\downarrow} \tag{3.6}$$

is obtained. The number operator defined as $n_{i\sigma} = b_{i\sigma}^{\dagger} b_{i\sigma}$. Because $[\mathcal{N}_{\sigma}, H] = 0$ where $\mathcal{N}_{\sigma} = \sum_i n_{i\sigma}$, the Hamiltonian has block diagonal form in number state basis.

3.2 Boundary Driven Model

In the previous section, the chain in which the transport will take place was defined. Now, we need to define particle reservoirs to drive current. Also, we need to introduce dephasing baths.

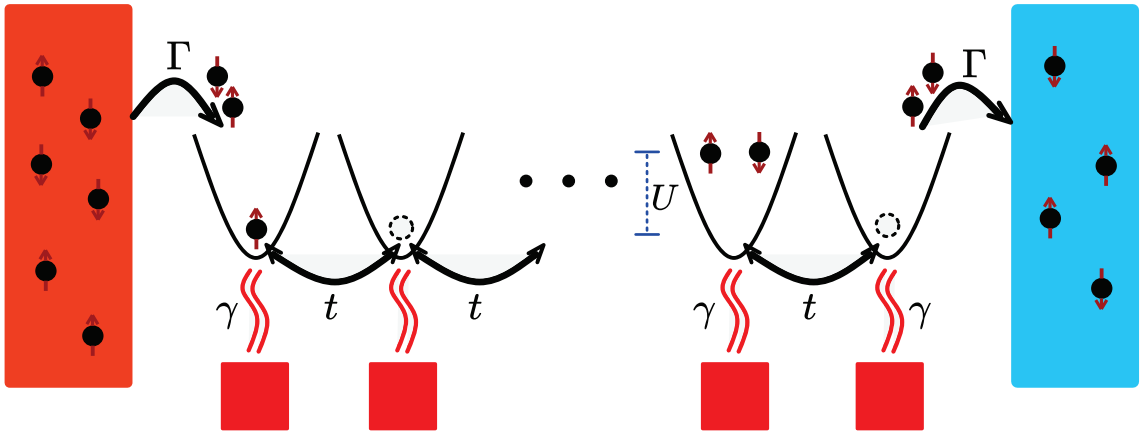

Figure 3.1: Schematic presentation of the boundary driven model.

As seen in Figure 3.1 two particle reservoirs coupled to the chain at the ends and each site coupled to independent baths which perform dephasing. The density matrix of

the system evolved according to the Lindblad equation setting $\hbar = 1$

$$\dot{\rho} = \mathcal{L}\rho = -i[H, \rho] + \mathcal{D}_{inj}[\rho] + \mathcal{D}_{ext}[\rho] + \mathcal{D}_{deph}[\rho] \tag{3.7}$$

where H is Fermi Hubbard Hamiltonian representing chain

$$H = -t \sum_{i}^{N-1} \sum_{\sigma} \left(b_{i\sigma}^{\dagger} b_{i+1,\sigma} + b_{i+1,\sigma}^{\dagger} b_{i\sigma} \right) + U \sum_{i}^{N} n_{i\uparrow} n_{i\downarrow}, \tag{3.8}$$

second term on the right-hand side represent left reservoir which coupled to first site, inject particle with injection rate Γ

$$\mathcal{D}_{inj}[\rho] = \Gamma \sum_{\sigma} \left(b_{1\sigma}^{\dagger} \rho b_{1\sigma} - \frac{1}{2} b_{1\sigma} b_{1\sigma}^{\dagger} \rho - \frac{1}{2} \rho b_{1\sigma} b_{1\sigma}^{\dagger} \right), \tag{3.9}$$

third term represent right reservoir which coupled to last site N, extract particle with extraction rate Γ

$$\mathcal{D}_{ext}[\rho] = \Gamma \sum_{\sigma} \left(b_{N\sigma} \rho b_{N\sigma}^{\dagger} - \frac{1}{2} b_{N\sigma}^{\dagger} b_{N\sigma} \rho - \frac{1}{2} \rho b_{N\sigma}^{\dagger} b_{N\sigma} \right) \tag{3.10}$$

and last term is dephasing term

$$\mathcal{D}_{deph}[\rho] = \gamma \sum_{i} \left(n_i \rho n_i - \frac{1}{2} n_i^2 \rho - \frac{1}{2} \rho n_i^2 \right) \tag{3.11}$$

where n_i is total particle operator defined as $n_i = n_{i\uparrow} + n_{i\downarrow}$.

This one-way driving represents low temperature limit or the case that potential difference between driving reservoirs are very high. Similar to the illustrative example in Equation (2.13) and more realistically, particle exchange with the reservoir must be two-way. The rates of this exchange are determined according to the Fermi Dirac distribution. Assuming the left reservoir has higher chemical potential and the right reservoir has lower chemical potential than the chain, low temperature T $\longrightarrow 0$ limit results one-way driving f $\longrightarrow 1$.

3.3 Particle Current Operator

Transport occurs as a result of the interaction of reservoirs at different temperatures or potentials, and when sufficient time passes, the system tends to enter a non-equilibrium steady state (NESS). Transport is characterized by a current. Using the continuity equation, the current operator is obtained. In the Heisenberg picture, the Lindblad master equation shown in Equation (2.8) become for operator $\mathcal{O}$

$$\frac{d}{dt}\mathcal{O} = \mathcal{L}^{\dagger}\mathcal{O} = i[H,\mathcal{O}] + \sum_k \gamma_k \left(L_k^{\dagger}\mathcal{O}L_k - \frac{1}{2}L_k^{\dagger}L_k\mathcal{O} - \frac{1}{2}\mathcal{O}L_k^{\dagger}L_k \right). \tag{3.12}$$

defining particle flux operator from site j to site j + 1

$$J_j := it\sum_{\sigma}\left(b_{j+1,\sigma}^{\dagger}b_{j\sigma} - b_{j\sigma}^{\dagger}b_{j+1,\sigma} \right), \quad 1 \leqslant j < N. \tag{3.13}$$

Using Equations (3.12) and (3.13), the continuity equation for site occupation

$$\frac{d}{dt}\langle n_j \rangle = \langle J_{j-1} \rangle - \langle J_j \rangle, \quad 1 < j < N \tag{3.14}$$

is obtained. Detailed calculations are found in Appendix A. At the boundaries, similar calculations result the continuity equations

$$\frac{d}{dt}\langle n_1\rangle = \langle J_{inj}\rangle - \langle J_1\rangle \tag{3.15}$$

$$\frac{d}{dt}\langle n_N\rangle = \langle J_{N-1}\rangle - \langle J_{ext}\rangle \tag{3.16}$$

where reservoir flux operators

$$J_{inj} = \Gamma\left(2 - n_1\right) \tag{3.17}$$

$$J_{ext} = \Gamma n_N \tag{3.18}$$

are defined. In the NESS, $\dot{n}_i$ = 0, and all the expectation of current operators are equal to each other

$$\langle J_{inj}\rangle = \langle J_1\rangle = ... = \langle J_{N-1}\rangle = \langle J_{ext}\rangle = \langle J\rangle. \tag{3.19}$$

CHAPTER 4

METHODS AND RESULTS

In this chapter, computational methods and result of the system dynamics are introduced. For the non-interacting chain, a highly effective exact solution method called the covariance matrix method is presented. For the interacting system, the mean-field approximation and improved approximate methods are described. The situations in which they were useful and the situations in which they failed were stated. The brute-force exact solution method used in most of the calculations throughout the thesis is described. In the last three sections, the behavior of current in an open quantum system is studied.

4.1 Non-Interacting Fermions

Sometimes, depending on the system and the features to be observed, a complete solution may not be necessary. An important group is systems in which the Hamiltonian is at most quadratic in the creation and annihilation operators. For the non-interacting case, as seen in Equation (3.6), the Hamiltonian become quadratic. In order to look at transport properties, the covariance matrix is defined as

$$C_{n,m}^{\sigma,\sigma'}(t) = Tr\{b_{n,\sigma}^{\dagger} b_{m,\sigma'} \rho(t)\} = \langle b_{n,\sigma}^{\dagger} b_{m,\sigma'} \rangle_t. \tag{4.1}$$

Using the Lindblad master equation in Heisenberg picture Equation (3.12), dynamics of covariance matrix

$$\begin{aligned} \dot{C}_{n,m}^{\sigma,\sigma'} = it(C_{n,m+1}^{\sigma,\sigma'} + C_{n,m-1}^{\sigma,\sigma'} - C_{n+1,m}^{\sigma,\sigma'} - C_{n-1,m}^{\sigma,\sigma'}) - \gamma(1-\delta_{nm})C_{n,m}^{\sigma,\sigma'} \\ - \frac{\Gamma}{2}(\delta_{1n} + \delta_{1m} + \delta_{Nn} + \delta_{Nm})C_{n,m}^{\sigma,\sigma'} + \Gamma\delta_{1n}\delta_{1m}\delta_{\sigma\sigma'} \end{aligned} \tag{4.2}$$

is obtained with open boundary conditions $C^{\sigma\sigma'}_{0,k} = C^{\sigma\sigma'}_{k,N+1} = 0$. The derivation of this equation can be found in Appendix A. With the help of vectorization, Equation (4.2) can be written as, $\dot{\mathbf{P}} = \mathbf{ZP} + \mathbf{D}$ where **P** is the vectorized covariance matrix. At the NESS, **P** = -$\mathbf{Z}^{-1}\mathbf{D}$. **Z** is a $4N^2 \times 4N^2$ matrix, with the computational cost of inversion of the most basic algorithm being $\mathcal{O}(N^6)$.

4.2 Mean-field Approximation

As shown in the previous section, the covariance matrix method for quadratic Hamiltonian provides a great advantage in calculations. However, when we take into account the interaction term which is quartic, the Hamiltonian cannot satisfy this condition. One of the simplest approximations for the Fermi-Hubbard model is the mean-field approximation. It converts the two-body interaction term to one-body interaction, which is between electron and mean-field of other electrons. Assuming the deviation of number operators from the mean value is relatively small,

$$n_{i\sigma} = \langle n_{i\sigma} \rangle + \delta n_{i\sigma} \tag{4.3}$$

interaction term of the Fermi Hubbard Hamiltonian Equation (3.6) become

$$\begin{aligned} U\sum_{i}^{N} n_{i,\uparrow} n_{i,\downarrow} &= U\sum_{i} (n_{i,\uparrow}\langle n_{i,\downarrow}\rangle + \langle n_{i,\uparrow}\rangle n_{i,\downarrow} - \langle n_{i,\uparrow}\rangle\langle n_{i,\downarrow}\rangle + \delta n_{i\uparrow}\delta n_{i\downarrow}) \\ &\approx U\sum_{i} (n_{i,\uparrow}\langle n_{i,\downarrow}\rangle + \langle n_{i,\uparrow}\rangle n_{i,\downarrow} - \langle n_{i,\uparrow}\rangle\langle n_{i,\downarrow}\rangle) \end{aligned} \tag{4.4}$$

where constant terms will be ignored. Now, dynamics of covariance matrix become

$$\begin{aligned} \dot{C}^{\sigma,\sigma'}_{n,m} = {} & it(C^{\sigma,\sigma'}_{n,m+1} + C^{\sigma,\sigma'}_{n,m-1} - C^{\sigma,\sigma'}_{n+1,m} - C^{\sigma,\sigma'}_{n-1,m}) + iU(C^{\tilde{\sigma},\tilde{\sigma}}_{n,n} - C^{\tilde{\sigma}',\tilde{\sigma}'}_{m,m})C^{\sigma,\sigma'}_{n,m} \\ & - \gamma(1-\delta_{nm})C^{\sigma,\sigma'}_{n,m} - \frac{\Gamma}{2}(\delta_{1n} + \delta_{1m} + \delta_{Nn} + \delta_{Nm})C^{\sigma,\sigma'}_{n,m} + \delta_{1,n}\delta_{1,m}\delta_{\sigma\sigma'}\Gamma \end{aligned} \tag{4.5}$$

with boundary conditions $C^{\sigma\sigma'}_{0,k} = C^{\sigma\sigma'}_{k,N+1} = 0$. Similarly to the non-interacting case with the help of vectorization, Equation (4.5) can be written as $\dot{\mathbf{P}} = \mathbf{Z(P)P} + \mathbf{D}$ where $\mathbf{P}$ is the vectorized covariance matrix. However, now coefficient matrix $\mathbf{Z}$ is depending on vectorized covariance matrix $\mathbf{P}$. It can be solved by non-linear system of equation methods or iterative methods.

One of the features which the mean-field approximation failed to describe is that current drops to zero exponentially with system size N in the interacting systems.[25] However, as seen in Figure 4.1a, the mean-field solution predicts ballistic behavior. On the other side, as seen in Figures 4.1b and 4.1c, it can be informative sometimes. Similarly to the exact solution, when the dephasing is at the order of the interaction strength, the current peaks.

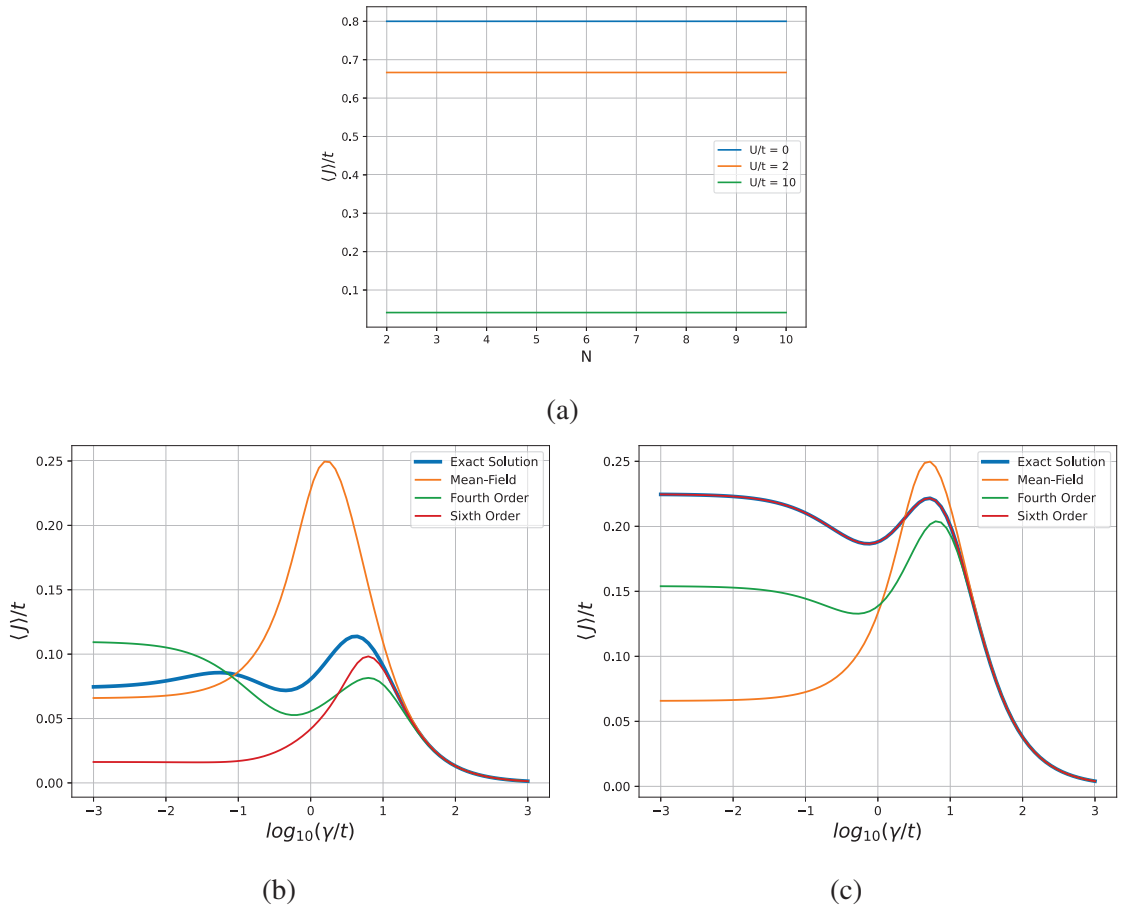

(a)

(b) (c)

Figure 4.1: Injection and extraction rates of system are Γ/t = 1 for both of the graphs. (a) Plots of the dependence of current $\langle J \rangle$ and the size of the system N for different interaction strengths U. Current is calculated using mean-field method. (b) Plots of current $\langle J \rangle$ vs dephasing rate γ of 4 site system with interaction strength U/t = 8. Currents are calculated using different methods. (c) Same plots of (b) for 2 site system.

4.3 Higher Order Approximations

The main problem of the interaction term is that it does not preserve the hierarchy of correlation functions. Applying the covariance matrix method to the interaction term, dynamics of second order correlation terms depend on fourth order correlation terms, fourth order correlation terms depend on sixth order correlation terms and goes on. However, by allowing higher-order correlation functions, we can get more accurate results. Now, let us introduce new notation

$$Q^{\prod_i \sigma_i \prod_j \sigma'_j}_{\prod_i n_i \prod_j m_j} := \langle \prod_i b^\dagger_{n_i \sigma_i} \prod_j b_{m_j \sigma'_j} \rangle \tag{4.6}$$

Dynamics of second and fourth order correlation functions are obtained as

$$\begin{aligned}
\frac{d}{dt} Q^{\sigma_1 \sigma'_1}_{n_1 m_1} &= it \left(Q^{\sigma_1, \sigma'_1}_{n_1, m_1+1} + Q^{\sigma_1, \sigma'_1}_{n_1, m_1-1} - Q^{\sigma_1, \sigma'_1}_{n_1-1, m_1} - Q^{\sigma_1, \sigma'_1}_{n_1+1, m_1} \right) - \gamma (1 - \delta_{n_1 m_1}) Q^{\sigma_1 \sigma'_1}_{n_1 m_1} \\
&+ iU \left(Q^{\uparrow\downarrow\downarrow\sigma'_1}_{n_1 n_1 n_1 m_1} \delta_{\uparrow\sigma_1} + Q^{\sigma_1 \downarrow\uparrow\downarrow}_{n_1 m_1 m_1 m_1} \delta_{\uparrow\sigma'_1} - Q^{\uparrow\downarrow\uparrow\sigma'_1}_{n_1 n_1 n_1 m_1} \delta_{\downarrow\sigma_1} - Q^{\sigma_1 \uparrow\uparrow\downarrow}_{n_1 m_1 m_1 m_1} \delta_{\downarrow\sigma'_1} \right) \\
&+ \Gamma \delta_{1 m_1} \delta_{1 n_1} \delta_{\sigma_1 \sigma'_1} - \frac{\Gamma}{2} (\delta_{1 n_1} + \delta_{1 m_1} + \delta_{N n_1} + \delta_{N m_1}) Q^{\sigma_1 \sigma'_1}_{n_1 m_1}
\end{aligned}$$

$$\begin{aligned}
\frac{d}{dt} Q^{\sigma_1 \sigma_2 \sigma'_1 \sigma'_2}_{n_1 n_2 m_1 m_2} &= it \left(Q^{\sigma_1 \sigma_2 \sigma'_1 \sigma'_2}_{n_1, n_2 m_1+1, m_2} + Q^{\sigma_1 \sigma_2 \sigma'_1 \sigma'_2}_{n_1, n_2 m_1-1, m_2} + Q^{\sigma_1 \sigma_2 \sigma'_1 \sigma'_2}_{n_1, n_2 m_1 m_2+1} + Q^{\sigma_1 \sigma_2 \sigma'_1 \sigma'_2}_{n_1, n_2 m_1 m_2-1} \right) \\
&- it \left(Q^{\sigma_1 \sigma_2 \sigma'_1 \sigma'_2}_{n_1+1, n_2 m_1 m_2} + Q^{\sigma_1 \sigma_2 \sigma'_1 \sigma'_2}_{n_1-1, n_2 m_1 m_2} + Q^{\sigma_1 \sigma_2 \sigma'_1 \sigma'_2}_{n_1 n_2+1, m_1 m_2} + Q^{\sigma_1 \sigma_2 \sigma'_1 \sigma'_2}_{n_1 n_2-1, m_1 m_2} \right) \\
&+ iU \left(\delta_{n_1 n_2} (1 - \delta_{\sigma_1 \sigma_2}) - \delta_{m_1 m_2} (1 - \delta_{\sigma'_1 \sigma'_2}) \right) Q^{\sigma_1 \sigma_2 \sigma'_1 \sigma'_2}_{n_1 n_2 m_1 m_2} \\
&+ iU \left(\delta_{\sigma_1 \downarrow} Q^{\uparrow\downarrow\sigma_2 \uparrow \sigma'_1 \sigma'_2}_{n_1 n_1 n_2 n_1 m_1 m_2} - \delta_{\sigma_1 \uparrow} Q^{\uparrow\downarrow\sigma_2 \downarrow \sigma'_1 \sigma'_2}_{n_1 n_1 n_2 n_1 m_1 m_2} + \delta_{\sigma_2 \uparrow} Q^{\uparrow\downarrow\sigma_1 \downarrow \sigma'_1 \sigma'_2}_{n_2 n_2 n_1 n_2 m_1 m_2} \right) \\
&- iU \left(\delta_{\sigma_2 \downarrow} Q^{\uparrow\downarrow\sigma_1 \uparrow \sigma'_1 \sigma'_2}_{n_2 n_2 n_1 n_2 m_1 m_2} - \delta_{\sigma'_1 \uparrow} Q^{\sigma_1 \sigma_2 \downarrow \sigma'_2 \uparrow\downarrow}_{n_1 n_2 m_1 m_2 m_1 m_1} + \delta_{\sigma'_1 \downarrow} Q^{\sigma_1 \sigma_2 \uparrow \sigma'_2 \uparrow\downarrow}_{n_1 n_2 m_1 m_2 m_1 m_1} \right) \\
&+ iU \left(\delta_{\sigma'_2 \downarrow} Q^{\sigma_1 \sigma_2 \uparrow \sigma'_1 \uparrow\downarrow}_{n_1 n_2 m_2 m_1 m_2 m_2} - \delta_{\sigma'_2 \uparrow} Q^{\sigma_1 \sigma_2 \downarrow \sigma'_1 \uparrow\downarrow}_{n_1 n_2 m_2 m_1 m_2 m_2} \right) - \Gamma \delta_{1 n_1} \delta_{1 m_1} \delta_{\sigma_1 \sigma'_1} Q^{\sigma_2 \sigma'_2}_{n_2 m_2} \\
&- \Gamma \delta_{1 n_2} \delta_{1 m_2} \delta_{\sigma_2 \sigma'_2} Q^{\sigma_1 \sigma'_1}_{n_1 m_1} + \Gamma \delta_{1 n_2} \delta_{1 m_1} \delta_{\sigma_2 \sigma'_1} Q^{\sigma_1 \sigma'_2}_{n_1 m_2} + \Gamma \delta_{1 n_1} \delta_{1 m_2} \delta_{\sigma_1 \sigma'_2} Q^{\sigma_2 \sigma'_1}_{n_2 m_1} \\
&- \frac{\Gamma}{2} (\delta_{N n_1} + \delta_{N n_2} + \delta_{N m_1} + \delta_{N m_2} + \delta_{1 n_1} + \delta_{1 n_2} + \delta_{1 m_1} + \delta_{1 m_2}) Q^{\sigma_1 \sigma_2 \sigma'_1 \sigma'_2}_{n_1 n_2 m_1 m_2} \\
&- \gamma (2 + \delta_{n_1 n_2} + \delta_{m_1 m_2} - \delta_{n_1 m_1} - \delta_{n_1 m_2} - \delta_{n_2 m_1} - \delta_{n_2 m_2}) Q^{\sigma_1 \sigma_2 \sigma'_1 \sigma'_2}_{n_1 n_2 m_1 m_2}.
\end{aligned} \tag{4.7}$$

Lastly dynamics of sixth order correlation functions while ignoring higher order terms

$$
\begin{aligned}
\frac{d}{dt}Q^{\sigma_1\sigma_2\sigma_3\sigma_1'\sigma_2'\sigma_3'}_{n_1n_2n_3m_1m_2m_3} &= it\left(Q^{\sigma_1\sigma_2\sigma_3\sigma_1'\sigma_2'\sigma_3'}_{n_1n_2n_3m_1+1,m_2m_3} + Q^{\sigma_1\sigma_2\sigma_3\sigma_1'\sigma_2'\sigma_3'}_{n_1n_2n_3m_1-1,m_2m_3} + Q^{\sigma_1\sigma_2\sigma_3\sigma_1'\sigma_2'\sigma_3'}_{n_1n_2n_3m_1m_2+1,m_3}\right) \\
&+ it\left(Q^{\sigma_1\sigma_2\sigma_3\sigma_1'\sigma_2'\sigma_3'}_{n_1n_2n_3m_1m_2-1,m_3} + Q^{\sigma_1\sigma_2\sigma_3\sigma_1'\sigma_2'\sigma_3'}_{n_1n_2n_3m_1m_2m_3+1} + Q^{\sigma_1\sigma_2\sigma_3\sigma_1'\sigma_2'\sigma_3'}_{n_1n_2n_3m_1m_2m_3-1}\right) \\
&- it\left(Q^{\sigma_1\sigma_2\sigma_3\sigma_1'\sigma_2'\sigma_3'}_{n_1+1,n_2n_3m_1m_2m_3} + Q^{\sigma_1\sigma_2\sigma_3\sigma_1'\sigma_2'\sigma_3'}_{n_1-1,n_2n_3m_1m_2m_3} + Q^{\sigma_1\sigma_2\sigma_3\sigma_1'\sigma_2'\sigma_3'}_{n_1n_2+1,n_3m_1m_2m_3}\right) \\
&- it\left(Q^{\sigma_1\sigma_2\sigma_3\sigma_1'\sigma_2'\sigma_3'}_{n_1n_2-1,n_3m_1m_2m_3} + Q^{\sigma_1\sigma_2\sigma_3\sigma_1'\sigma_2'\sigma_3'}_{n_1n_2n_3+1,m_1m_2m_3} + Q^{\sigma_1\sigma_2\sigma_3\sigma_1'\sigma_2'\sigma_3'}_{n_1n_2n_3-1,m_1m_2m_3}\right) \\
&+ iU\left(\delta_{n_1n_2}(1-\delta_{\sigma_1\sigma_2}) + \delta_{n_1n_3}(1-\delta_{\sigma_1\sigma_3})\right) Q^{\sigma_1\sigma_2\sigma_3\sigma_1'\sigma_2'\sigma_3'}_{n_1n_2n_3m_1m_2m_3} \\
&+ iU\left(\delta_{n_2n_3}(1-\delta_{\sigma_2\sigma_3}) - \delta_{m_1m_2}(1-\delta_{\sigma_1'\sigma_2'})\right) Q^{\sigma_1\sigma_2\sigma_3\sigma_1'\sigma_2'\sigma_3'}_{n_1n_2n_3m_1m_2m_3} \\
&- iU\left(\delta_{m_1m_3}(1-\delta_{\sigma_1'\sigma_3'}) + \delta_{m_2m_3}(1-\delta_{\sigma_2'\sigma_3'})\right) Q^{\sigma_1\sigma_2\sigma_3\sigma_1'\sigma_2'\sigma_3'}_{n_1n_2n_3m_1m_2m_3} \\
&+ \Gamma\delta_{1n_1}\delta_{1m_1}\delta_{\sigma_1\sigma_1'}Q^{\sigma_2\sigma_3\sigma_2'\sigma_3'}_{n_2n_3m_2m_3} - \Gamma\delta_{1n_1}\delta_{1m_2}\delta_{\sigma_1\sigma_2'}Q^{\sigma_2\sigma_3\sigma_1'\sigma_3'}_{n_2n_3m_1m_3} \\
&+ \Gamma\delta_{1n_1}\delta_{1m_3}\delta_{\sigma_1\sigma_3'}Q^{\sigma_2\sigma_3\sigma_1'\sigma_2'}_{n_2n_3m_1m_2} - \Gamma\delta_{1n_2}\delta_{1m_1}\delta_{\sigma_2\sigma_1'}Q^{\sigma_1\sigma_3\sigma_2'\sigma_3'}_{n_1n_3m_2m_3} \\
&+ \Gamma\delta_{1n_2}\delta_{1m_2}\delta_{\sigma_2\sigma_2'}Q^{\sigma_1\sigma_3\sigma_1'\sigma_3'}_{n_1n_3m_1m_3} - \Gamma\delta_{1n_2}\delta_{1m_3}\delta_{\sigma_2\sigma_3'}Q^{\sigma_1\sigma_3\sigma_1'\sigma_2'}_{n_1n_3m_1m_2} \\
&+ \Gamma\delta_{1n_3}\delta_{1m_1}\delta_{\sigma_3\sigma_1'}Q^{\sigma_1\sigma_2\sigma_2'\sigma_3'}_{n_1n_2m_2m_3} - \Gamma\delta_{1n_3}\delta_{1m_2}\delta_{\sigma_3\sigma_2'}Q^{\sigma_1\sigma_2\sigma_1'\sigma_3'}_{n_1n_2m_1m_3} \\
&+ \Gamma\delta_{1n_3}\delta_{1m_3}\delta_{\sigma_3\sigma_3'}Q^{\sigma_1\sigma_2\sigma_1'\sigma_2'}_{n_1n_2m_1m_2} \\
&- \frac{\Gamma}{2}(\delta_{1n_1}+\delta_{1n_2}+\delta_{1n_3}+\delta_{1m_1}+\delta_{1m_2}+\delta_{1m_3})Q^{\sigma_1\sigma_2\sigma_3\sigma_1'\sigma_2'\sigma_3'}_{n_1n_2n_3m_1m_2m_3} \\
&- \frac{\Gamma}{2}(\delta_{Nn_1}+\delta_{Nn_2}+\delta_{Nn_3}+\delta_{Nm_1}+\delta_{Nm_2}+\delta_{Nm_3})Q^{\sigma_1\sigma_2\sigma_3\sigma_1'\sigma_2'\sigma_3'}_{n_1n_2n_3m_1m_2m_3} \\
&- \gamma\left(3+\delta_{m_1m_2}+\delta_{m_1m_3}+\delta_{m_2m_3}\right) Q^{\sigma_1\sigma_2\sigma_3\sigma_1'\sigma_2'\sigma_3'}_{n_1n_2n_3m_1m_2m_3} \\
&- \gamma\left(\delta_{n_1n_2}+\delta_{n_1n_3}+\delta_{n_2n_3}\right) Q^{\sigma_1\sigma_2\sigma_3\sigma_1'\sigma_2'\sigma_3'}_{n_1n_2n_3m_1m_2m_3} \\
&- \gamma\left(\delta_{m_1n_1}+\delta_{m_1n_2}+\delta_{m_1n_3}\right) Q^{\sigma_1\sigma_2\sigma_3\sigma_1'\sigma_2'\sigma_3'}_{n_1n_2n_3m_1m_2m_3} \\
&- \gamma\left(\delta_{m_2n_1}+\delta_{m_2n_2}+\delta_{m_2n_3}\right) Q^{\sigma_1\sigma_2\sigma_3\sigma_1'\sigma_2'\sigma_3'}_{n_1n_2n_3m_1m_2m_3} \\
&- \gamma\left(\delta_{m_3n_1}+\delta_{m_3n_2}+\delta_{m_3n_3}\right) Q^{\sigma_1\sigma_2\sigma_3\sigma_1'\sigma_2'\sigma_3'}_{n_1n_2n_3m_1m_2m_3}
\end{aligned}
\tag{4.8}
$$

is obtained. Derivation of the equations can be found in Appendix B. As seen in Figures 4.1b and 4.1c, even only holding up to fourth-order correlations, it makes a great improvement over the mean-field solution. It is a good approach, both qualitatively and quantitatively. However, there is a relationship between system size and error here. In Figure 4.1c, the use of up to sixth-order correlation functions gives the same result as the exact solution for the two-site system. The problem of the sixth-order equation is that,

although the error is small, it does not provide much speed advantage on the computation side. There are $(2N)^4$ fourth-order correlation functions and $(2N)^6$ sixth-order correlation functions. For this reason, the computational cost of the forth-order method is $\mathcal{O}(N^{12})$ and sixth-order method is $\mathcal{O}(N^{18})$. Figure 4.1b shows that the sixth-order correlation method is not better than the fourth-order correlation methods for all regimes.

4.4 Exact Solution

The most basic approach to an exact solution is using number states as basis. The main problem is that the density matrix of the N site system has 2^{4N} elements. Inside the chain, the number of spin-up and spin-down particles is conserved. At the boundaries, non-unitary dynamics of injection and extraction do not cause superposition of states which have different number of spin-up or spin-down particle. So, the density matrix will be block diagonal for different spin-up and spin-down states. Now, only $\sum_{i=0}^{N}\sum_{j=0}^{N}\left(\binom{N}{i}\binom{N}{j}\right)^2$ elements are needed for solution of the density matrix.

4.5 Transport Regimes

System size dependence of the current is an important classification in transport problems. When system size N is big enough, current has the form

$$J \propto \frac{1}{N^{\nu}} \tag{4.9}$$

where ν is transport coefficient and N is number of site. Different values of ν represents different transport regimes, as seen in Table 4.1. It can also be determined by spreading of a localized wave-packet, but we preferred using current for simplicity.With the help of linear fitting and logarithm of Equation (4.9)

$$lnJ = -\nu lnN + C \tag{4.10}$$

Table 4.1: Classification of transport regime with respect to exponent ν
(Source: Lacerda, A.M. (2020). Transport in boundary-driven quantum chains with quasiperiodic potentials (p. 63)).

Transport regime	Transport coefficient
Ballistic	$\nu = 0$
Super-diffusive	$0 < \nu < 1$
Diffusive	$\nu = 1$
Sub-diffusive	$\nu > 1$
Localized	$\nu = \infty$

ν is found. When transport is coherent, the non-interacting Fermi Hubbard chain is in the ballistic regime.[26] However, introducing dephasing changes this and the system goes from ballistic to localized regime continuously with increasing dephasing as seen in Figure 4.2.

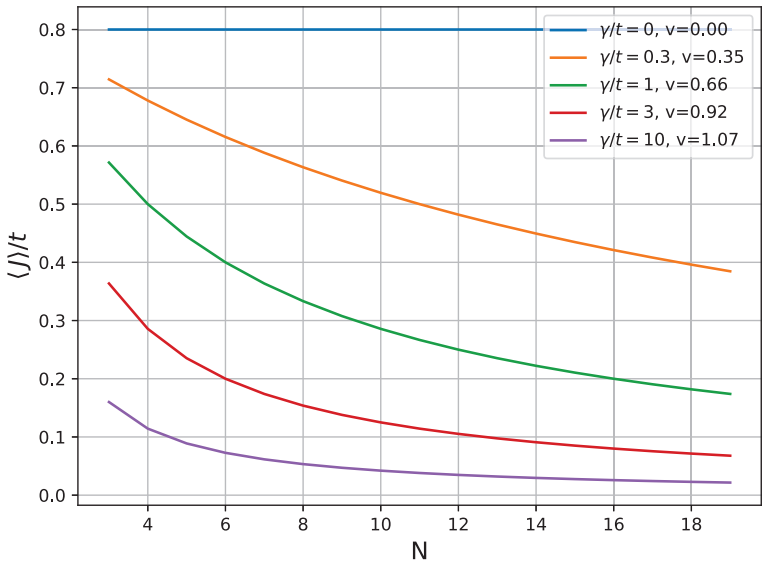

Figure 4.2: Plots of current $\langle J \rangle$ and system size N dependence in non-interacting system (U=0) for different dephasing rate γ with corresponding fitted transport coefficient ν. Injection and extraction rates of system are Γ/t = 1.

4.6 Effects of Environment

Like unitary quantum dynamics, non-unitary quantum dynamics behaves differently from its classical counterpart. Boundary driven quantum chain that is represented in Equation (3.7) has two different kind of baths.

One of them is particle reservoirs which is parameterized by Γ, inject and extract particles. In Figure 4.3, behavior of the current with respect to driving rate Γ for different interaction strength U is shown. Intuitively, one would expect that increasing the injection and extraction rate will increase the current up to a limit and the increase will stop after saturation is reached. However, unlike the classical model, current shows non-monotonic behavior because of the quantum Zeno effect. Injection from reservoir or extraction to reservoir can be thought of as indirect continuous monitoring of the system, and this leads to the Zeno effect. When interaction strength is high enough, two local maximum of current appear. In the $\Gamma \gg t$ limit, regardless of interaction strength, they all converge to the same value because the Zeno effect dominates.

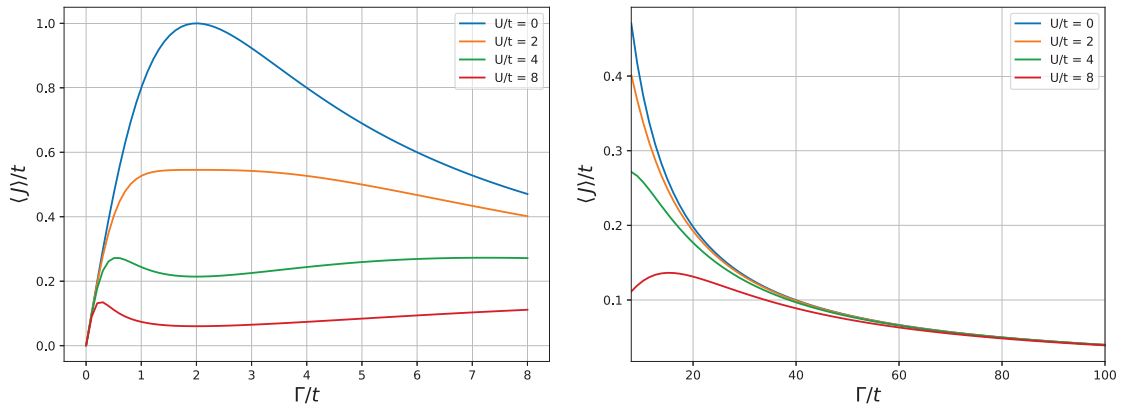

Figure 4.3: Plots of current $\langle J \rangle$ vs dephasing rate γ of 4 site system with injection rate $\Gamma/t = 1$ for different interaction strength U. (a) Driving rate is in the range $\Gamma \in$ [0,8], (b) Driving rate is in the range $\Gamma \in$ [8,100].

Other important bath effects are caused by dephasing baths that are coupled to each site and are parameterized by γ. In the Figure 4.4, it is shown that how current changes with respect to dephasing. Injection rate Γ is chosen equal to hopping rate in a 4 site system. The vast majority of non-interacting, many body systems show ballistic transport. It was shown that dephasing causes transition from ballistic to diffusive regime in the Figure 4.2 for non-interacting system. Therefore, dephasing always negatively affects transport in

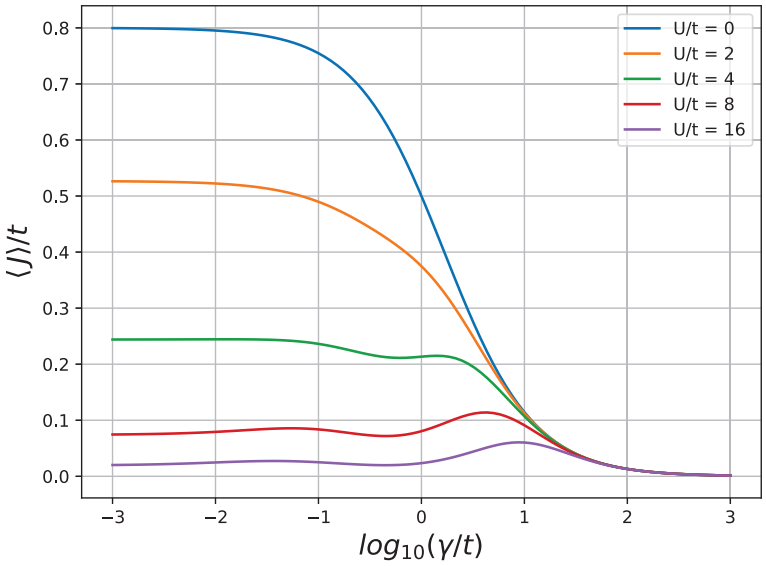

Figure 4.4: Plots of current $\langle J \rangle$ vs dephasing rate γ of 4 site system with injection rate $\Gamma/t = 1$ for different interaction strength U.

these systems. For non-interacting case and relatively small interaction strength, e.g. U/t = 2, this negative effect is seen in Figure 4.4. However, strongly correlated systems do not show this feature and the effects of dephasing are different. For spinless many-body systems, enhancement of dephasing on transport is shown.[27] As seen in Figure 4.4, also for the Fermi-Hubbard model, there is a current-increasing effect up to a level, for high interaction strengths.

4.7 Enhancement Mechanism

The main result of this thesis is that bulk dephasing can enhance the transport in the strongly correlated system. Figure 4.5a shows this behavior in detail for the system of 4 sites with U / t = 8. Important dephasing values are marked. These values are used throughout this section to explain this striking behavior.

As mentioned in Chapter 3, the Hamiltonian of the system conserves the number of spin-up and spin-down particles. This means that all spin sectors are decoupled from each other. The transition between spin sectors is achieved through the injection and extraction of particles at the ends of the chain. Driving part couple spin sector ($n_\downarrow$,$n_\uparrow$) to ($n_\downarrow \pm 1$,$n_\uparrow$) and ($n_\downarrow$,$n_\uparrow \pm 1$) where n_σ represents the number of spin-σ particles. Since Lindblad equation of the system Equation (3.7) has spin symmetry, spin-down was chosen to explain the mechanism.

Defining configuration states as

$$|n_{1\downarrow}, n_{2\downarrow}, ..., n_{N\downarrow}\rangle \otimes |n_{1\uparrow}, n_{2\uparrow}, ..., n_{N\uparrow}\rangle \tag{4.11}$$

where number of spin-σ particle on site i, $n_{i\sigma}$ take values 0 or 1. The states in the form $|1, x, 0\rangle \otimes |y\rangle$ are decoupled from the spin-down driving, where x and y are any string of bits of length N-2 and N, respectively. These decoupled states are called dark states, and the weight of the dark states determines the current. To determine the weight of the dark states, the darksity operator for spin-down D is defined as

$$D := n_{1\downarrow}(1 - n_{N\downarrow}). \tag{4.12}$$

As shown in,[25] all particles are frozen in the first half of the chain in the NESS. Because of that, the current is suppressed. Therefore, the system prefers to populate high energy dark states and spin sector (N/2,N/2), it is seen in Figure 4.6d.

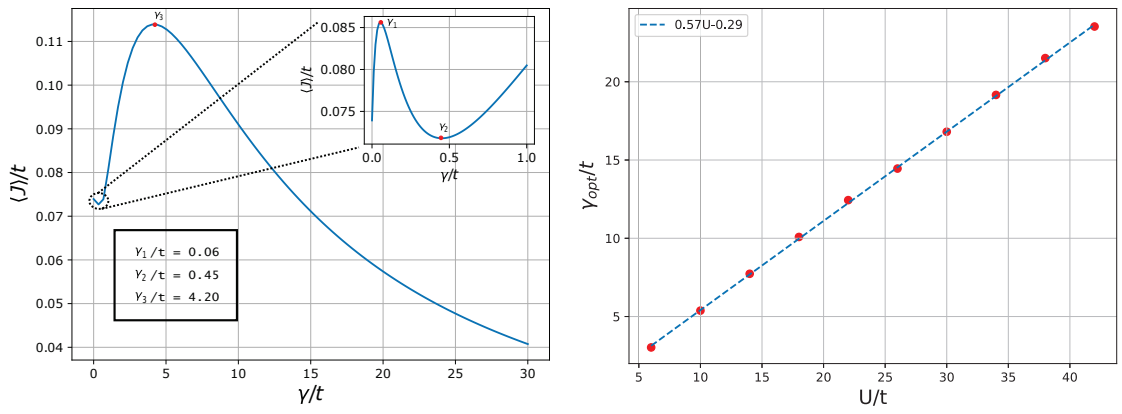

(a) (b)

Figure 4.5: (a) Plots of current $\langle J \rangle$ vs dephasing rate γ of 4 site system with driving rate $\Gamma/t = 1$ and interaction strength U/t = 1. Important dephasing values are marked. Inset Figure: More detailed drawing of the same figure in the range $\gamma \in [0, 1]$. (b) Plots of the interaction strength U vs optimal dephasing γ_{opt} of 4 sites system with driving rate $\Gamma/t = 1$.

Let us consider U/t $\rightarrow \infty$ limit for better understanding. The hopping term in the Hamiltonian Equation (3.6) can be ignored, and only the interaction term survives. Configuration states become eigenstates of this Hamiltonian. Each eigenstate in the same band has the same energy and determined by the number of double occupied sites. Bands are separated by U. Since all particles are frozen in the first half of the chain in the NESS, they will populate dark states in the form

$$|\underbrace{1,1,...,1}_{n_\downarrow},\underbrace{0,0,...,0}_{N-n_\downarrow}\rangle \otimes |\underbrace{1,1,...,1}_{n_\uparrow},\underbrace{0,0,...,0}_{N-n_\uparrow}\rangle \tag{4.13}$$

for the spin sector ($n_\downarrow$,$n_\uparrow$) eigenstates. They are maximally double occupied, therefore they are in the highest energy band.

Taking a step forward, let us consider a finite but strong interaction limit. Taking hopping term as perturbation, degenerate eigenstates will split because of hopping. This leads to that band gap will be order of U and energy splitting inside the bands will be order of t^2/2U. In Figure 4.6a, this behavior can be observed. Similar to $U/t \rightarrow \infty$ limit, it is obvious that dark states population will be dominated by highest energy band.

When dephasing is introduced to the system, dephasing process induce scattering between the eigenstates of the Hamiltonian. The energy of the system will fluctuate. Because dephasing operator does not commute with the hopping term, on average there is a loss of energy associated with kinetic energy. Using Equation (3.7), the effect of dephasing on energy of the system

$$\frac{d}{dt}\langle H\rangle = -2\gamma t \sum_{j=1}^{N}\sum_{\sigma}\langle b_{j\sigma}^\dagger b_{j+1,\sigma} + b_{j+1,\sigma}^\dagger b_{j\sigma}\rangle + ... \tag{4.14}$$

is determined. There is an inverse proportionality between the terms on the right-hand side. Increase dephasing leads to decrease in kinetic energy because of the quantum Zeno effect. So, there is an optimum dephasing rate for enhancement.

Looking closely at the spin sector (2,2) which is the highest populated sector for 4 sites system, it is seen that the scattering between eigenstates is due to dephasing in Figure 4.6. Scattering to more mobile states causes current enhancement. It is seen that the dephasing rate that causes the transition between eigenstates is related to the energy

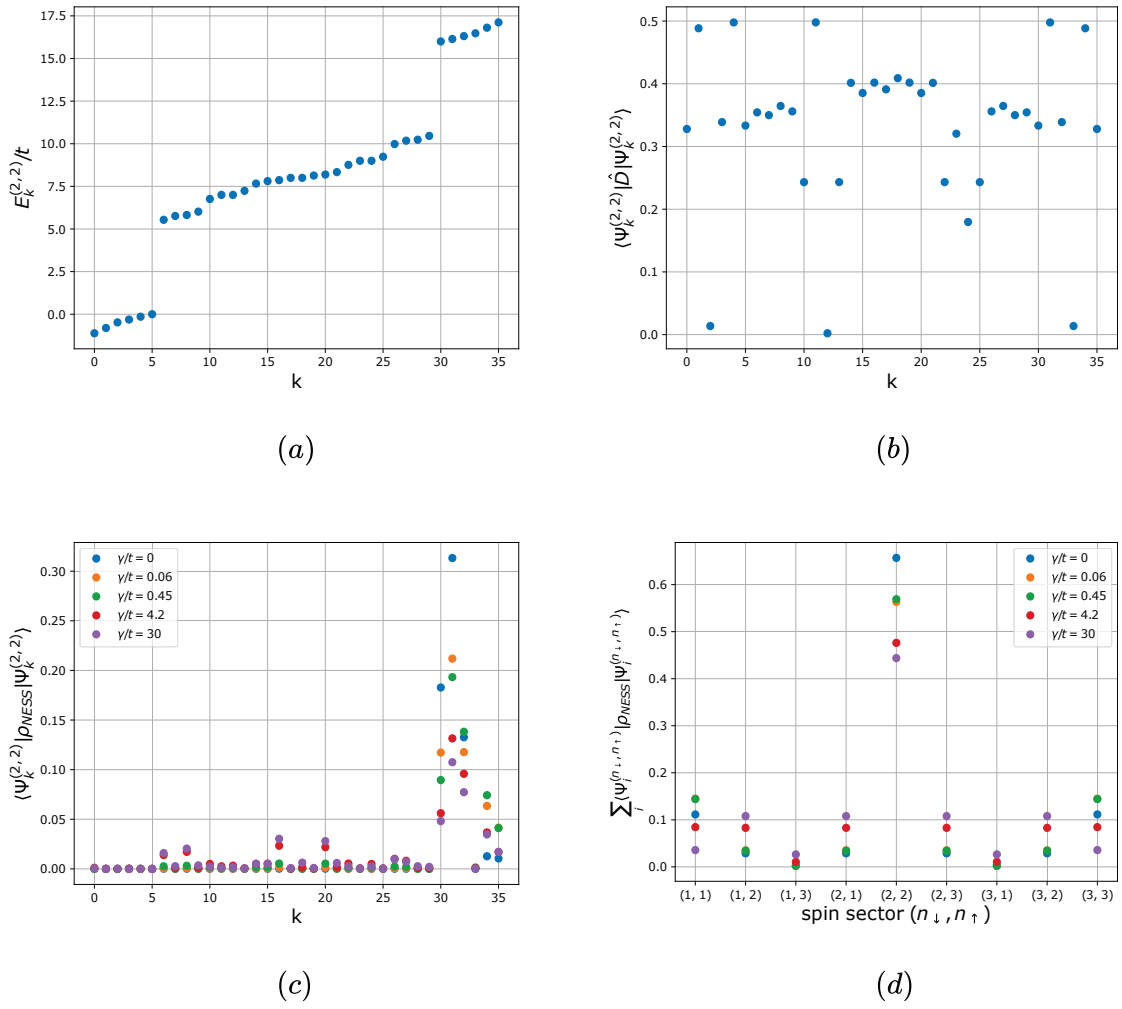

(a) (b) (c) (d)

Figure 4.6: Eigenstates of the Hamiltonian in the spin number sector (2,2) $\Psi_k^{(2,2)}$ for N = 4 and U/t = 8 are calculated. Each eigenstate indexed with number k. Also in this chain, steady state density matrix ρ_{NESS} is calculated with driving rate $\Gamma/t = 1$ for different dephasing rates γ. (a) The energy spectrum of the eigenstates. (b) Weight of dark states in the eigenstates. (c) Weight of eigenstates in the steady state density matrix ρ_{NESS}. (d) Weight of spin sectors in the steady state density matrix ρ_{NESS}.

difference between these eigenstates. In Figure 4.5b, this relation is shown for band gap. There is a linear dependence between interaction strength U and optimal dephasing γ_{opt} which causes maximum current. For small dephasing rate, jumps are observed to be more dominant in the higher band. As indicated in Figure 4.5a, there is a local maximum for dephasing value $\gamma_{deph}/t = 0.06$. However, satisfactory observation could not be made regarding the relation between enhancement in the lower dephasing values and energy difference between states in the same band. In addition to scattering between states in the same spin sector, spin sector populations are also changes because of dephasing as seen in Figure 4.6d. The combination of these effects changes the dark state population and, accordingly, the current.

CHAPTER 5

CONCLUSION

In this thesis, transport properties of the interacting and non-interacting fermions on 1D chains under environmental effects are studied. Since, the main challenge of the many-body systems is exponentially growing Hilbert space and as a result, the computational cost, different solution methods are introduced. Their advantages and weaknesses are shown. It was concluded that the mean-field approximation has an enormous speed advantage and helps to understand the behavior of the system in certain regimes. However, the mean-field method is error-prone at some points. The higher order correlation method is more accurate and very effective in understanding the behavior of the system. However, because the higher order correlation methods have high polynomial complexity while exact solution has exponential complexity, speed advantage compared to the mean-field method is slight for small system size.

It was shown that dephasing change ballistic behavior of the transport of the non-interacting fermions to diffusive behavior. In contrast to this negative effect seen in the non-interacting systems, current enhancement is observed in the interacting systems. In the absence of dephasing, increasing interaction reduces the current, but when the system is under the effect of dephasing, it has been shown to affect the current positively at some points. The mechanism behind this behavior is explained with the Hamiltonian energy spectrum. In this direction, the relation between the band gap and the optimal dephasing values are found. One of the most important shortcomings of this study and its potential for improvement is that only small systems can be investigated. Increasing system size will require more advanced computational methods, e.g. tensor network, matrix product states. It will help us understand the mechanism behind these effects and learn whether they depend on the size of the system. As a result, the mechanism that attempts to explain this behavior of the current is open to support and development with advanced analytical or computational methods.

APPENDIX A

DYNAMICS OF THE COVARIANCE MATRIX

In this chapter, derivation of the dynamical equation of the covariance matrix is introduced. Dynamics of the covariance matrix is obtained by the equation

$$\dot{C}^{\sigma\sigma'}_{nm} = \frac{d}{dt}\langle b^{\dagger}_{n\sigma} b_{m\sigma'}\rangle = i\langle[H, b^{\dagger}_{n\sigma} b_{m\sigma'}]\rangle + Tr\{b^{\dagger}_{n\sigma} b_{m\sigma'}\mathcal{D}(\rho)\} \tag{A.1}$$

where $\mathcal{D}(\rho)$ represent the non-unitary part of the Lindblad equation. Thanks to mean-field approximation, the system Hamiltonian H is quadratic. The general form of the Hamiltonian H can be expressed as

$$H = \sum H^{ss'}_{ij} b^{\dagger}_{is} b_{js'} \tag{A.2}$$

where $H^{ss'}_{ij} = -t\delta_{ss'}(\delta_{i,j-1} + \delta_{i,j+1}) + U\langle n_{i\tilde{s}}\rangle\delta_{ij}\delta_{ss'}$. Using following two equations

$$\begin{aligned}
[b^{\dagger}_{is} b_{js'}, b^{\dagger}_{n\sigma}] &= b^{\dagger}_{is} b_{js'} b^{\dagger}_{n\sigma} - b^{\dagger}_{n\sigma} b^{\dagger}_{is} b_{js'} \\
&= b^{\dagger}_{is}\{b_{js'}, b^{\dagger}_{n\sigma}\} \\
&= b^{\dagger}_{is}\delta_{jn}\delta_{s'\sigma}
\end{aligned} \tag{A.3}$$

$$\begin{aligned}
[b^{\dagger}_{is} b_{js'}, b_{m\sigma'}] &= b^{\dagger}_{is} b_{js'} b_{m\sigma'} - b_{m\sigma'} b^{\dagger}_{is} b_{js'} \\
&= -\{b_{m\sigma'}, b^{\dagger}_{is}\} b_{js'} \\
&= -b_{js'}\delta_{mi}\delta_{s\sigma'}
\end{aligned} \tag{A.4}$$

and the following calculations

$$
\begin{aligned}
[H, b^\dagger_{n\sigma} b_{m\sigma'}] &= [H, b^\dagger_{n\sigma}] b_{m\sigma'} + b^\dagger_{n\sigma} [H, b_{m\sigma'}] \\
&= \sum_{ijss'} H^{ss'}_{ij} \left([b^\dagger_{is} b_{js'}, b^\dagger_{n\sigma}] b_{m\sigma'} + b^\dagger_{n\sigma} [b^\dagger_{is} b_{js'}, b_{m\sigma'}] \right) \\
&= \sum_{is} H^{s\sigma}_{in} b^\dagger_{is} b_{m\sigma'} - \sum_{js'} H^{\sigma' s'}_{mj} b^\dagger_{n\sigma} b_{js'} \\
&= \sum_{is} \left(-t\delta_{s\sigma} (\delta_{i,n-1} + \delta_{i,n+1}) + U \langle n_{i\tilde{s}} \rangle \delta_{in} \delta_{s\sigma} \right) b^\dagger_{is} b_{m\sigma'} \\
&+ \sum_{js'} (t\delta_{s'\sigma'} (\delta_{m,j-1} + \delta_{m,j+1}) - U \langle n_{m\tilde{\sigma}'} \rangle \delta_{mj} \delta_{s'\sigma'}) b^\dagger_{n\sigma} b_{js'} \\
&= t(b^\dagger_{n\sigma} b_{m+1,\sigma'} + b^\dagger_{n\sigma} b_{m-1,\sigma'} - b^\dagger_{n-1,\sigma} b_{m\sigma'} - b^\dagger_{n+1,\sigma} b_{m\sigma'}) \\
&+ U \left(\langle n_{n\tilde{\sigma}} \rangle - \langle n_{m\tilde{\sigma}'} \rangle \right) b^\dagger_{n\sigma} b_{m\sigma'}
\end{aligned}
\tag{A.5}
$$

coherent evolution of covariance matrix is obtained as

$$
\dot{C}^{\sigma,\sigma'}_{n,m} = it(C^{\sigma,\sigma'}_{n,m+1} + C^{\sigma,\sigma'}_{n,m-1} - C^{\sigma,\sigma'}_{n+1,m} - C^{\sigma,\sigma'}_{n-1,m}) + iU(C^{\tilde{\sigma},\tilde{\sigma}}_{n,n} - C^{\tilde{\sigma}',\tilde{\sigma}'}_{m,m}) C^{\sigma,\sigma'}_{n,m} \tag{A.6}
$$

To obtain the equation of dissipative evolution, the following identity will be useful:

$$
\begin{aligned}
\langle A \mathcal{D}_k(\rho) \rangle &= Tr\{ A L_k \rho L^\dagger_k - \frac{1}{2} A L^\dagger_k L_k \rho - \frac{1}{2} A \rho L^\dagger_k L_k \} \\
&= \frac{1}{2} \langle L^\dagger_k [A, L_k] \rangle - \frac{1}{2} \langle [A, L^\dagger_k] L_k \rangle
\end{aligned}
\tag{A.7}
$$

Contribution of injection part with the help of Equations (A.3), (A.4) and (A.7)

$$\begin{aligned}
\langle b^\dagger_{n\sigma} b_{m\sigma'} \mathcal{D}_{inj}(\rho)\rangle &= \frac{\Gamma}{2}\sum_s \Big(\langle b_{1s}[b^\dagger_{n\sigma} b_{m\sigma'}, b^\dagger_{1s}]\rangle - \langle [b^\dagger_{n\sigma} b_{m\sigma'}, b_{1s}] b^\dagger_{1s}\rangle\Big) \\
&= \frac{\Gamma}{2}\sum_s \Big(\delta_{1m}\delta_{s\sigma'}\langle b_{1s} b^\dagger_{n\sigma}\rangle + \delta_{1n}\delta_{s\sigma}\langle b_{m\sigma'} b^\dagger_{1s}\rangle\Big) \\
&= \frac{\Gamma}{2}\Big(\delta_{1m}\langle b_{1\sigma'} b^\dagger_{n\sigma}\rangle + \delta_{1n}\langle b_{m\sigma'} b^\dagger_{1\sigma}\rangle\Big) \\
&= \frac{\Gamma}{2}\Big(\delta_{1m}\langle \delta_{1n}\delta_{\sigma\sigma'} - b^\dagger_{n\sigma} b_{1\sigma'}\rangle + \delta_{1n}\langle \delta_{1m}\delta_{\sigma\sigma'} - b^\dagger_{1\sigma} b_{m\sigma'}\rangle\Big) \\
&= \Gamma\delta_{1n}\delta_{1m}\delta_{\sigma\sigma'} - \frac{\Gamma}{2}(\delta_{1n} + \delta_{1m})\langle b^\dagger_{n\sigma} b_{m\sigma'}\rangle \\
&= \Gamma\delta_{1n}\delta_{1m}\delta_{\sigma\sigma'} - \frac{\Gamma}{2}(\delta_{1n} + \delta_{1m}) C^{\sigma\sigma'}_{nm}
\end{aligned} \tag{A.8}$$

and extraction part

$$\begin{aligned}
\langle b^\dagger_{n\sigma} b_{m\sigma'} \mathcal{D}_{ext}(\rho)\rangle &= \frac{\Gamma}{2}\sum_s \Big(\langle b^\dagger_{Ns}[b^\dagger_{n\sigma} b_{m\sigma'}, b_{Ns}]\rangle - \langle [b^\dagger_{n\sigma} b_{m\sigma'}, b^\dagger_{Ns}] b_{Ns}\rangle\Big) \\
&= -\frac{\Gamma}{2}\sum_s \Big(\delta_{Nn}\delta_{s\sigma}\langle b^\dagger_{Ns} b_{m\sigma'}\rangle + \delta_{Nm}\delta_{s\sigma'}\langle b^\dagger_{n\sigma} b_{Ns}\rangle\Big) \\
&= -\frac{\Gamma}{2}(\delta_{Nn} + \delta_{Nm})\langle b^\dagger_{n\sigma} b_{m\sigma'}\rangle \\
&= -\frac{\Gamma}{2}(\delta_{Nn} + \delta_{Nm}) C^{\sigma\sigma'}_{nm}
\end{aligned} \tag{A.9}$$

is obtained. Lastly, with the help of the following relation

$$\begin{aligned}
\Big[b^\dagger_{n\sigma} b_{m\sigma'}, n_i\Big] &= \Big[b^\dagger_{n\sigma} b_{m\sigma'}, \sum_s b^\dagger_{is} b_{is}\Big] \\
&= \sum_s \Big(b^\dagger_{is}[b^\dagger_{n\sigma} b_{m\sigma'}, b_{is}] + [b^\dagger_{n\sigma} b_{m\sigma}, b^\dagger_{is}]\Big) \\
&= \sum_s \Big(-b^\dagger_{is} b_{m\sigma'}\delta_{in}\delta_{s\sigma} + b^\dagger_{ns} b_{is}\delta_{im}\delta_{s\sigma'}\Big) \\
&= (\delta_{im} - \delta_{in}) b^\dagger_{n\sigma} b_{m\sigma'}
\end{aligned} \tag{A.10}$$

and Equations (A.7), (A.10) and the hermiticity of the corresponding dephasing Lindblad operator n_i, dephasing part

$$\begin{aligned}
\langle b^\dagger_{n\sigma} b_{m\sigma'} \mathcal{D}_{deph}(\rho)\rangle &= \frac{\gamma}{2}\sum_{i=1}^{N}\langle n_i[b^\dagger_{n\sigma} b_{m\sigma'}, n_i] - [b^\dagger_{n\sigma} b_{m\sigma'}, n_i]n_i\rangle \\
&= \frac{\gamma}{2}\sum_{i}\langle n_i(\delta_{im}-\delta_{in})b^\dagger_{n\sigma} b_{m\sigma'} - (\delta_{im}-\delta_{in})b^\dagger_{n\sigma} b_{m\sigma'}n_i\rangle \\
&= -\frac{\gamma}{2}\sum_{i}(\delta_{im}-\delta_{in})\langle[b^\dagger_{n\sigma} b_{m\sigma'}, n_i]\rangle \\
&= -\frac{\gamma}{2}\sum_{i}(\delta_{im}-\delta_{in})^2\langle b^\dagger_{n\sigma} b_{m\sigma'}\rangle \\
&= -\gamma(1-\delta_{nm})\langle b^\dagger_{n\sigma} b_{n\sigma'}\rangle \\
&= -\gamma(1-\delta_{nm})C^{\sigma\sigma'}_{nm}
\end{aligned} \tag{A.11}$$

is obtained. When all the results are combined, dynamics of the covariance matrix Equation (4.2) is obtained.

APPENDIX B

HIERARCHY OF EQUATION

In this chapter, hierarchic dynamical equation of higher order correlation functions are derived. Now, let us define new notations;

$$C^{\prod_i \sigma_i}_{\prod_i n_i} := \prod_i b^\dagger_{n_i\sigma_i} \tag{B.1}$$

$$A^{\prod_j \sigma'_j}_{\prod_j m_j} := \prod_j b_{m_j\sigma'_j} \tag{B.2}$$

$$Q^{\prod_i \sigma_i \prod_j \sigma'_j}_{\prod_i n_i \prod_j m_j} := \langle \prod_i b^\dagger_{n_i\sigma_i} \prod_j b_{m_j\sigma'_j} \rangle_\infty \tag{B.3}$$

with boundary conditions which, if any of the sub indices is equal to zero or N+1, $Q^{\prod_i \sigma_i \prod_j \sigma'_j}_{\prod_i n_i \prod_j m_j}$ is equal to zero. Also, let us introduce useful equivalences which are used throughout this chapter.

$$[C^{\sigma_1\sigma_2}_{n_1n_2}, b^\dagger_{is}] = b^\dagger_{n_1\sigma_1} b^\dagger_{n_2\sigma_2} b^\dagger_{is} - b^\dagger_{is} b^\dagger_{n_1\sigma_1} b^\dagger_{n_2\sigma_2} = 0 \tag{B.4}$$

$$[A^{\sigma'_1\sigma'_2}_{m_1m_2}, b_{js'}] = b_{m_1\sigma'_1} b_{m_2\sigma'_2} b_{js'} - b_{js'} b_{m_1\sigma'_1} b_{m_2\sigma'_2} b_{js'} = 0 \tag{B.5}$$

$$
\begin{aligned}
[A^{\sigma_1'\sigma_2'}_{m_1m_2}, b^\dagger_{is}] &= b_{m_1\sigma_1'} b_{m_2\sigma_2'} b^\dagger_{is} - b^\dagger_{is} b_{m_1\sigma_1'} b_{m_2\sigma_2'} \\
&= b_{m_1\sigma_1'}(\delta_{im_2}\delta_{s\sigma_2'} - b^\dagger_{is} b_{m_2\sigma_2'}) - b^\dagger_{is} b_{m_1\sigma_1'} b_{m_2\sigma_2'} \\
&= \delta_{im_2}\delta_{s\sigma_2'} b_{m_1\sigma_1'} - (\delta_{im_1}\delta_{s\sigma_1'} - b^\dagger_{is} b_{m_1\sigma_1'}) b_{m_2\sigma_2'} - b^\dagger_{is} b_{m_1\sigma_1'} b_{m_2\sigma_2'} \\
&= \delta_{im_2}\delta_{s\sigma_2'} b_{m_1\sigma_1'} - \delta_{im_1}\delta_{s\sigma_1'} b_{m_2\sigma_2'}
\end{aligned}
\tag{B.6}
$$

$$
\begin{aligned}
[C^{\sigma_1\sigma_2}_{n_1n_2}, b_{js'}] &= b^\dagger_{n_1\sigma_1} b^\dagger_{n_2\sigma_2} b_{js'} - b_{js'} b^\dagger_{n_1\sigma_1} b^\dagger_{n_2\sigma_2} \\
&= b^\dagger_{n_1\sigma_1}(\delta_{jn_2}\delta_{s'\sigma_2} - b_{js'} b^\dagger_{n_2\sigma_2}) - b_{js'} b^\dagger_{n_1\sigma_1} b^\dagger_{n_2\sigma_2} \\
&= \delta_{jn_2}\delta_{s'\sigma_2} b^\dagger_{n_1\sigma_1} - (\delta_{jn_1}\delta_{s'\sigma_1} - b_{js'} b^\dagger_{n_1\sigma_1}) b^\dagger_{n_2\sigma_2} - b_{js'} b^\dagger_{n_1\sigma_1} b^\dagger_{n_2\sigma_2} \\
&= \delta_{jn_2}\delta_{s'\sigma_2} b^\dagger_{n_1\sigma_1} - \delta_{jn_1}\delta_{s'\sigma_1} b^\dagger_{n_2\sigma_2}
\end{aligned}
\tag{B.7}
$$

$$
\begin{aligned}
[A^{\sigma_1'\sigma_2'}_{m_1m_2}, C^{\sigma_1\sigma_2}_{n_1n_2}] &= b_{m_1\sigma_1'}[b_{m_2\sigma_2'}, C^{\sigma_1\sigma_2}_{n_1n_2}] + [b_{m_1\sigma_1'}, C^{\sigma_1\sigma_2}_{n_1n_2}] b_{m_2\sigma_2'} \\
&= b_{m_1\sigma_1'} b^\dagger_{n_2\sigma_2}\delta_{n_1m_2}\delta_{\sigma_1\sigma_2'} - b_{m_1\sigma_1'} b^\dagger_{n_1\sigma_1}\delta_{n_2m_2}\delta_{\sigma_2\sigma_2'} \\
&+ b^\dagger_{n_2\sigma_2} b_{m_2\sigma_2'}\delta_{n_1m_1}\delta_{\sigma_1\sigma_1'} - b^\dagger_{n_1\sigma_1} b_{m_2\sigma_2'}\delta_{n_2m_1}\delta_{\sigma_2\sigma_1'} \\
&= b^\dagger_{n_1\sigma_1} b_{m_1\sigma_1'}\delta_{n_2m_2}\delta_{\sigma_2\sigma_2'} + b^\dagger_{n_2\sigma_2} b_{m_2\sigma_2'}\delta_{n_1m_1}\delta_{\sigma_1\sigma_1'} \\
&- b^\dagger_{n_1\sigma_1} b_{m_2\sigma_2'}\delta_{n_2m_1}\delta_{\sigma_2\sigma_1'} - b^\dagger_{n_2\sigma_2} b_{m_1\sigma_1'}\delta_{n_1m_2}\delta_{\sigma_1\sigma_2'} \\
&+ \delta_{n_2m_1}\delta_{\sigma_2\sigma_1'}\delta_{n_1m_2}\delta_{\sigma_1\sigma_2'} - \delta_{n_1m_1}\delta_{\sigma_1\sigma_1'}\delta_{n_2m_2}\delta_{\sigma_2\sigma_2'}
\end{aligned}
\tag{B.8}
$$

$$
\begin{aligned}
[n_i, A^{\sigma_1'\sigma_2'}_{m_1m_2}] &= \sum_s [b^\dagger_{is} b_{is}, A^{\sigma_1'\sigma_2'}_{m_1m_2}] \\
&= \sum_s (A^{\sigma_2's}_{m_2i}\delta_{im_1}\delta_{s\sigma_1'} - A^{\sigma_1's}_{m_1i}\delta_{im_2}\delta_{s\sigma_2'}) \\
&= -(\delta_{im_1} + \delta_{im_2}) A^{\sigma_1'\sigma_2'}_{m_1m_2}
\end{aligned}
\tag{B.9}
$$

$$
[n_i, C^{\sigma_1\sigma_2}_{n_1n_2}] = (\delta_{in_1} + \delta_{in_2}) C^{\sigma_1\sigma_2}_{n_1n_2} \tag{B.10}
$$

Now all the tools which are required are introduced. Let us start with the second order equation. It is already obtained in Appendix A except interaction part. The interaction term can be written in normal order as $n_{i\uparrow}n_{i\downarrow} = -C^{\uparrow\downarrow}_{ii} A^{\uparrow\downarrow}_{ii}$ and its contribution obtained

as

$$\begin{aligned}\sum_i [C_{ii}^{\uparrow\downarrow} A_{ii}^{\uparrow\downarrow}, b_{n_1\sigma_1}^\dagger b_{m_1\sigma_1'}] &= \sum_i (C_{ii}^{\uparrow\downarrow} [A_{ii}^{\uparrow\downarrow}, b_{n_1\sigma_1}^\dagger b_{m_1\sigma_1'}] + [C_{ii}^{\uparrow\downarrow}, b_{n_1\sigma_1}^\dagger b_{m_1\sigma_1'}] A_{ii}^{\uparrow\downarrow}) \\ &= \sum_i (C_{ii}^{\uparrow\downarrow} [A_{ii}^{\uparrow\downarrow}, b_{n_1\sigma_1}^\dagger] b_{m_1\sigma_1'} + b_{n_1\sigma_1}^\dagger [C_{ii}^{\uparrow\downarrow}, b_{m_1\sigma_1'}] A_{ii}^{\uparrow\downarrow}) \\ &= \sum_i (C_{ii}^{\uparrow\downarrow} A_{im_1}^{\uparrow\sigma_1'} \delta_{in_1} \delta_{\downarrow\sigma_1} - C_{ii}^{\uparrow\downarrow} A_{im_1}^{\downarrow\sigma_1'} \delta_{in_1} \delta_{\uparrow\sigma_1} \\ &+ C_{n_1 i}^{\sigma_1\uparrow} A_{ii}^{\uparrow\downarrow} \delta_{im_1} \delta_{\downarrow\sigma_1'} - C_{n_1 i}^{\sigma_1\downarrow} A_{ii}^{\uparrow\downarrow} \delta_{im_1} \delta_{\uparrow\sigma_1'}) \\ &= C_{n_1 n_1}^{\uparrow\downarrow} A_{n_1 m_1}^{\uparrow\sigma_1'} \delta_{\downarrow\sigma_1} - C_{n_1 n_1}^{\uparrow\downarrow} A_{n_1 m_1}^{\downarrow\sigma_1'} \delta_{\uparrow\sigma_1} \\ &+ C_{n_1 m_1}^{\sigma_1\uparrow} A_{m_1 m_1}^{\uparrow\downarrow} \delta_{\downarrow\sigma_1'} - C_{n_1 m_1}^{\sigma_1\downarrow} A_{m_1 m_1}^{\uparrow\downarrow} \delta_{\uparrow\sigma_1'}\end{aligned} \tag{B.11}$$

so, adding the interaction part to the equation which is obtained in Appendix A, Equation (4.7) is derived.

Proceeding to the fourth order equation. Starting from contribution of the hopping term,

$$\begin{aligned}\Big\langle \sum_{i,s} [b_{i+1,s}^\dagger b_{is} + h.c, C_{n_1 n_2}^{\sigma_1\sigma_2} A_{m_1 m_2}^{\sigma_1'\sigma_2'}] \Big\rangle &= \Big\langle \sum_{i,s} (C_{n_1 n_2}^{\sigma_1\sigma_2} [b_{i+1,s}^\dagger b_{is} + b_{is}^\dagger b_{i+1,s}, A_{m_1 m_2}^{\sigma_1'\sigma_2'}] \\ &+ [b_{i+1,s}^\dagger b_{is} + b_{is}^\dagger b_{i+1,s}, C_{n_1 n_2}^{\sigma_1\sigma_2}] A_{m_1 m_2}^{\sigma_1'\sigma_2'}) \Big\rangle \\ &= \Big\langle \sum_{i,s} (C_{n_1 n_2}^{\sigma_1\sigma_2} A_{m_2 i}^{\sigma_2' s} \delta_{i+1,m_1} \delta_{s\sigma_1'} \\ &- C_{n_1 n_2}^{\sigma_1\sigma_2} A_{m_1 i}^{\sigma_1' s} \delta_{i+1,m_2} \delta_{s\sigma_2'} \\ &+ C_{n_1 n_2}^{\sigma_1\sigma_2} A_{m_2 i+1}^{\sigma_2' s} \delta_{i,m_1} \delta_{s\sigma_1'} - C_{n_1 n_2}^{\sigma_1\sigma_2} A_{m_1 i+1}^{\sigma_1' s} \delta_{i,m_2} \delta_{s\sigma_2'} \\ &+ C_{i+1,n_2}^{s\sigma_2} A_{m_1 m_2}^{\sigma_1'\sigma_2'} \delta_{in_1} \delta_{s\sigma_1} - C_{i+1,n_1}^{s\sigma_1} A_{m_1 m_2}^{\sigma_1'\sigma_2'} \delta_{in_2} \delta_{s\sigma_2} \\ &+ C_{in_2}^{s\sigma_2} A_{m_1 m_2}^{\sigma_1'\sigma_2'} \delta_{i+1,n_1} \delta_{s\sigma_1} - C_{in_1}^{s\sigma_1} A_{m_1 m_2}^{\sigma_1'\sigma_2'} \delta_{i+1,n_2} \delta_{s\sigma_2}) \Big\rangle \\ &= Q_{n_1+1,n_2 m_1 m_2}^{\sigma_1\sigma_2\sigma_1'\sigma_2'} + Q_{n_1-1,n_2 m_1 m_2}^{\sigma_1\sigma_2\sigma_1'\sigma_2'} + Q_{n_1 n_2+1,m_1 m_2}^{\sigma_1\sigma_2\sigma_1'\sigma_2'} \\ &+ Q_{n_1 n_2-1,m_1 m_2}^{\sigma_1\sigma_2\sigma_1'\sigma_2'} - Q_{n_1,n_2 m_1+1,m_2}^{\sigma_1\sigma_2\sigma_1'\sigma_2'} - Q_{n_1,n_2 m_1-1,m_2}^{\sigma_1\sigma_2\sigma_1'\sigma_2'} \\ &- Q_{n_1,n_2 m_1 m_2+1}^{\sigma_1\sigma_2\sigma_1'\sigma_2'} - Q_{n_1,n_2 m_1 m_2-1}^{\sigma_1\sigma_2\sigma_1'\sigma_2'}\end{aligned} \tag{B.12}$$

then, interaction term

$$
\begin{aligned}
\langle\sum_i[C_{ii}^{\uparrow\downarrow}A_{ii}^{\uparrow\downarrow},C_{n_1n_2}^{\sigma_1\sigma_2}A_{m_1m_2}^{\sigma_1'\sigma_2'}]\rangle &= \langle\sum_i(C_{ii}^{\uparrow\downarrow}[A_{ii}^{\uparrow\downarrow},C_{n_1n_2}^{\sigma_1\sigma_2}]A_{m_1m_2}^{\sigma_1'\sigma_2'}+C_{n_1n_2}^{\sigma_1\sigma_2}[C_{ii}^{\uparrow\downarrow},A_{m_1m_2}^{\sigma_1'\sigma_2'}]A_{ii}^{\uparrow\downarrow})\rangle \\
&= \langle\sum_i(C_{ii}^{\uparrow\downarrow}(b_{n_1\sigma_1}^\dagger b_{i\uparrow}\delta_{in_2}\delta_{\downarrow\sigma_2}+b_{n_2\sigma_2}^\dagger b_{i\downarrow}\delta_{in_1}\delta_{\uparrow\sigma_1})A_{m_1m_2}^{\sigma_1'\sigma_2'} \\
&- C_{ii}^{\uparrow\downarrow}(b_{n_1\sigma_1}^\dagger b_{i\downarrow}\delta_{n_2i}\delta_{\sigma_2\uparrow}+b_{n_2\sigma_2}^\dagger b_{i\uparrow}\delta_{n_1i}\delta_{\sigma_1\downarrow})A_{m_1m_2}^{\sigma_1'\sigma_2'} \\
&+ C_{ii}^{\uparrow\downarrow}(\delta_{in_1}\delta_{\sigma_1\downarrow}\delta_{in_2}\delta_{\sigma_2\uparrow}-\delta_{in_1}\delta_{\sigma_1\uparrow}\delta_{in_2}\delta_{\sigma_2\downarrow})A_{m_1m_2}^{\sigma_1'\sigma_2'} \\
&- C_{n_1n_2}^{\sigma_1\sigma_2}(b_{i\uparrow}^\dagger b_{m_1\sigma_1'}\delta_{im_2}\delta_{\downarrow\sigma_2'}+b_{i\downarrow}^\dagger b_{m_2\sigma_2'}\delta_{im_1}\delta_{\uparrow\sigma_1'})A_{ii}^{\uparrow\downarrow} \\
&+ C_{n_1n_2}^{\sigma_1\sigma_2}(b_{i\uparrow}^\dagger b_{m_2\sigma_2'}\delta_{im_1}\delta_{\downarrow\sigma_1'}+b_{i\downarrow}^\dagger b_{m_1\sigma_1'}\delta_{im_2}\delta_{\uparrow\sigma_2'})A_{ii}^{\uparrow\downarrow} \\
&+ C_{n_1n_2}^{\sigma_1\sigma_2}(\delta_{im_1}\delta_{im_2}\delta_{\uparrow\sigma_1'}\delta_{\downarrow\sigma_2'}-\delta_{im_1}\delta_{im_2}\delta_{\downarrow\sigma_1'}\delta_{\uparrow\sigma_2'})A_{ii}^{\uparrow\downarrow})\rangle \\
&= Q_{n_2n_2n_1n_2m_1m_2}^{\uparrow\downarrow\sigma_1\uparrow\sigma_1'\sigma_2'}\delta_{\sigma_2\downarrow}+Q_{n_1n_1n_2n_1m_1m_2}^{\uparrow\downarrow\sigma_2\downarrow\sigma_1'\sigma_2'}\delta_{\sigma_1\uparrow} \\
&- Q_{n_2n_2n_1n_2m_1m_2}^{\uparrow\downarrow\sigma_1\downarrow\sigma_1'\sigma_2'}\delta_{\sigma_2\uparrow}-Q_{n_1n_1n_2n_1m_1m_2}^{\uparrow\downarrow\sigma_2\uparrow\sigma_1'\sigma_2'}\delta_{\sigma_1\downarrow} \\
&- Q_{n_1n_2m_1m_2}^{\sigma_1\sigma_2\sigma_1'\sigma_2'}\delta_{n_1n_2}(1-\delta_{\sigma_1\sigma_2})-Q_{n_1n_2m_2m_1m_2m_2}^{\sigma_1\sigma_2\uparrow\sigma_1'\uparrow\downarrow}\delta_{\sigma_2'\downarrow} \\
&- Q_{n_1n_2m_1m_2m_1m_1}^{\sigma_1\sigma_2\downarrow\sigma_2'\uparrow\downarrow}\delta_{\sigma_1'\uparrow}+Q_{n_1n_2m_1m_2m_1m_1}^{\sigma_1\sigma_2\uparrow\sigma_2'\uparrow\downarrow}\delta_{\sigma_1'\downarrow} \\
&+ Q_{n_1n_2m_2m_1m_2m_2}^{\sigma_1\sigma_2\downarrow\sigma_1'\uparrow\downarrow}\delta_{\sigma_2'\uparrow}+Q_{n_1n_2m_1m_2}^{\sigma_1\sigma_2\sigma_1'\sigma_2'}\delta_{m_1m_2}(1-\delta_{\sigma_1'\sigma_2'})
\end{aligned}
\tag{B.13}
$$

For injection term, following four identity is introduced.

$$
\begin{aligned}
\langle\delta_{1m_2}b_{m_2\sigma_2'}b_{n_1\sigma_1}^\dagger b_{n_2\sigma_2}^\dagger b_{m_1\sigma_1'}\rangle &= \langle\delta_{1m_2}(\delta_{n_1m_2}\delta_{\sigma_1\sigma_2'}-b_{n_1\sigma_1}^\dagger b_{m_2\sigma_2'})b_{n_2\sigma_2}^\dagger b_{m_1\sigma_1'}\rangle \\
&= \langle\delta_{1m_2}\delta_{1n_1}\delta_{\sigma_1\sigma_2'}b_{n_2\sigma_2}^\dagger b_{m_1\sigma_1'} \\
&- \delta_{1m_2}b_{n_1\sigma_1}^\dagger(\delta_{n_2m_2}\delta_{\sigma_2\sigma_2'}-b_{n_2\sigma_2}^\dagger b_{m_2\sigma_2'})b_{m_1\sigma_1'}\rangle \\
&= \delta_{1m_2}\delta_{1n_1}\delta_{\sigma_1\sigma_2'}Q_{n_2m_1}^{\sigma_2\sigma_1'}-\delta_{1m_2}\delta_{1n_2}\delta_{\sigma_2\sigma_2'}Q_{n_1m_1}^{\sigma_1\sigma_1'} \\
&- \delta_{1m_2}Q_{n_1n_2m_1m_2}^{\sigma_1\sigma_2\sigma_1'\sigma_2'}
\end{aligned}
\tag{B.14}
$$

applying $(m_1, m_2) = (m_2, m_1)$ and $(\sigma_1', \sigma_2') = (\sigma_2', \sigma_1')$ transformation to Equation (B.14),

$$\langle \delta_{1m_1} b_{m_1} b^\dagger_{n_1} b^\dagger_{n_2} b_{m_2} \rangle = \delta_{1m_1}\delta_{1n_1}\delta_{\sigma_1\sigma_1'} Q^{\sigma_2\sigma_2'}_{n_2m_2} - \delta_{1m_1}\delta_{1n_2}\delta_{\sigma_2\sigma_1'} Q^{\sigma_1\sigma_2'}_{n_1m_2} + \delta_{1m_1} Q^{\sigma_1\sigma_2\sigma_1'\sigma_2'}_{n_1n_2m_1m_2} \tag{B.15}$$

is obtained.

$$\begin{aligned}
\langle \delta_{1n_2} b^\dagger_{n_1\sigma_1} b_{m_1\sigma_1'} b_{m_2\sigma_2'} b^\dagger_{n_2\sigma_2} \rangle &= \langle \delta_{1n_2} b^\dagger_{n_1\sigma_1} b_{m_1\sigma_1'} (\delta_{n_2m_2}\delta_{\sigma_2\sigma_2'} - b^\dagger_{n_2\sigma_2} b_{m_2\sigma_2'}) \rangle \\
&= \langle \delta_{1n_2}\delta_{1m_2}\delta_{\sigma_2\sigma_2'} b^\dagger_{n_1\sigma_1} b_{m_1\sigma_1'} \\
&- \delta_{1n_2} b^\dagger_{n_1\sigma_1} (\delta_{n_2m_1}\delta_{\sigma_2\sigma_1'} - b^\dagger_{n_2\sigma_2} b_{m_1\sigma_1'}) b_{m_2\sigma_2'} \rangle \\
&= \delta_{1n_2}\delta_{1m_2}\delta_{\sigma_2\sigma_2'} Q^{\sigma_1\sigma_1'}_{n_1m_1} - \delta_{1n_2}\delta_{1m_1}\delta_{\sigma_2\sigma_1'} Q^{\sigma_1\sigma_2'}_{n_1m_2} \\
&+ \delta_{1n_2} Q^{\sigma_1\sigma_2\sigma_1'\sigma_2'}_{n_1n_2m_1m_2}
\end{aligned} \tag{B.16}$$

applying $(n_1, n_2) = (n_2, n_1)$ and $(\sigma_1, \sigma_2) = (\sigma_2, \sigma_1)$ transformation to Equation (B.16)

$$\begin{aligned}
\langle \delta_{1n_1} b^\dagger_{n_2\sigma_2} b_{m_1\sigma_1'} b_{m_2\sigma_2'} b^\dagger_{n_1\sigma_1} \rangle &= \delta_{1n_1}\delta_{1m_2}\delta_{\sigma_1\sigma_2'} Q^{\sigma_2\sigma_1'}_{n_2m_1} \\
&- \delta_{1n_1}\delta_{1m_1}\delta_{\sigma_1\sigma_1'} Q^{\sigma_2\sigma_2'}_{n_2m_2} - \delta_{1n_1} Q^{\sigma_1\sigma_2\sigma_1'\sigma_2'}_{n_1n_2m_1m_2}
\end{aligned} \tag{B.17}$$

is obtained. Using Equations (B.14) - (B.17), injection part leads to following equation

$$\begin{aligned}
\langle C^{\sigma_1\sigma_2}_{n_1n_2} A^{\sigma'_1\sigma'_2}_{m_1m_2} \mathcal{D}_{inj} \rangle &= \frac{\Gamma}{2} \sum_s (\langle b_{1s} [C^{\sigma_1\sigma_2}_{n_1n_2} A^{\sigma'_1\sigma'_2}_{m_1m_2}, b^\dagger_{1s}] \rangle - \langle [C^{\sigma_1\sigma_2}_{n_1n_2} A^{\sigma'_1\sigma'_2}_{m_1m_2}, b_{1s}] b^\dagger_{1s} \rangle) \\
&= \frac{\Gamma}{2} \sum_s (\langle b_{1s} C^{\sigma_1\sigma_2}_{n_1n_2} [A^{\sigma'_1\sigma'_2}_{m_1m_2}, b^\dagger_{1s}] \rangle - \langle [C^{\sigma_1\sigma_2}_{n_1n_2}, b_{1s}] A^{\sigma'_1\sigma'_2}_{m_1m_2} b^\dagger_{1s} \rangle) \\
&= \frac{\Gamma}{2} \sum_s (\langle b_{1s} C^{\sigma_1\sigma_2}_{n_1n_2} (b_{m_1\sigma'_1} \delta_{1m_2} \delta_{s\sigma'_2} - b_{m_2\sigma'_2} \delta_{1m_1} \delta_{s\sigma'_1}) \rangle \\
&- \langle (b^\dagger_{n_1\sigma_1} \delta_{1n2} \delta_{s\sigma_2} - b^\dagger_{n_2\sigma_2} \delta_{1n_1} \delta_{s\sigma_1}) A^{\sigma'_1\sigma'_2}_{m_1m_2} b^\dagger_{1s} \rangle) \\
&= \frac{\Gamma}{2} (\langle b_{m_2\sigma'_2} C^{\sigma_1\sigma_2}_{n_1n_2} b_{m_1\sigma'_1} \rangle \delta_{1m_2} - \langle b_{m_1\sigma'_1} C^{\sigma_1\sigma_2}_{n_1n_2} b_{m_2\sigma'_2} \rangle \delta_{1m_1} \\
&- \langle b^\dagger_{n_1\sigma_1} A^{\sigma'_1\sigma'_2}_{m_1m_2} b^\dagger_{n_2\sigma_2} \rangle \delta_{1n_2} + \langle b^\dagger_{n_2\sigma_2} A^{\sigma'_1\sigma'_2}_{m_1m_2} b^\dagger_{n_1\sigma_1} \rangle \delta_{1n_1}) \\
&= -\Gamma \delta_{1n_2} \delta_{1m_2} \delta_{\sigma_2\sigma'_2} Q^{\sigma_1\sigma'_1}_{n_1m_1} + \Gamma \delta_{1n_2} \delta_{1m_1} \delta_{\sigma_2\sigma'_1} Q^{\sigma_1\sigma'_2}_{n_1m_2} \\
&+ \Gamma \delta_{1n_1} \delta_{1m_2} \delta_{\sigma_1\sigma'_2} Q^{\sigma_2\sigma'_1}_{n_2m_1} - \Gamma \delta_{1n_1} \delta_{1m_1} \delta_{\sigma_1\sigma'_1} Q^{\sigma_2\sigma'_2}_{n_2m_2} \\
&- \frac{\Gamma}{2} (\delta_{1n_1} + \delta_{1n_2} + \delta_{1m_1} + \delta_{1m_2}) Q^{\sigma_1\sigma_2\sigma'_1\sigma'_2}_{n_1n_2m_1m_2}
\end{aligned} \tag{B.18}$$

extraction part

$$\begin{aligned}
\langle C^{\sigma_1\sigma_2}_{n_1n_2} A^{\sigma'_1\sigma'_2}_{m_1m_2} \mathcal{D}_{ext} \rangle &= \frac{\Gamma}{2} \sum_s (\langle b^\dagger_{Ns} [C^{\sigma_1\sigma_2}_{n_1n_2} A^{\sigma'_1\sigma'_2}_{m_1m_2}, b_{Ns}] \rangle - \langle [C^{\sigma_1\sigma_2}_{n_1n_2} A^{\sigma'_1\sigma'_2}_{m_1m_2}, b^\dagger_{Ns}] b_{Ns} \rangle) \\
&= \frac{\Gamma}{2} \sum_s (\langle b^\dagger_{Ns} [C^{\sigma_1\sigma_2}_{n_1n_2}, b_{Ns}] A^{\sigma'_1\sigma'_2}_{m_1m_2} \rangle - \langle C^{\sigma_1\sigma_2}_{n_1n_2} [A^{\sigma'_1\sigma'_2}_{m_1m_2}, b^\dagger_{Ns}] b_{Ns} \rangle) \\
&= \frac{\Gamma}{2} \sum_s (\delta_{Nn_2} \delta_{s\sigma_2} Q^{s\sigma_1\sigma'_1\sigma'_2}_{Nn_1m_1m_2} - \delta_{Nn_1} \delta_{s\sigma_1} Q^{s\sigma_2\sigma'_1\sigma'_2}_{Nn_2m_1m_2} \\
&- \delta_{Nm_2} \delta_{s\sigma'_2} Q^{\sigma_1\sigma_2\sigma'_1 s}_{n_1n_2m_1N} + \delta_{Nm_1} \delta_{s\sigma'_1} Q^{\sigma_1\sigma_2\sigma'_2 s}_{n_1n_2m_2N}) \\
&= \frac{\Gamma}{2} (\delta_{Nn_2} Q^{\sigma_2\sigma_1\sigma'_1\sigma'_2}_{n_2n_1m_1m_2} - \delta_{Nn_1} Q^{\sigma_1\sigma_2\sigma'_1\sigma'_2}_{n_1n_2m_1m_2} \\
&- \delta_{Nm_2} Q^{\sigma_1\sigma_2\sigma'_1\sigma'_2}_{n_1n_2m_1m_2} + \delta_{Nm_1} Q^{\sigma_1\sigma_2\sigma'_2\sigma'_1}_{n_1n_2m_2m_1}) \\
&= -\frac{\Gamma}{2} (\delta_{Nn_1} + \delta_{Nn_2} + \delta_{Nm_1} + \delta_{Nm_2}) Q^{\sigma_1\sigma_2\sigma'_1\sigma'_2}_{n_1n_2m_1m_2}
\end{aligned} \tag{B.19}$$

Lastly, contribution from dephasing term can be calculated using Equations (B.9) and

(B.10)

$$\begin{aligned}
\langle C^{\sigma_1\sigma_2}_{n_1n_2} A^{\sigma_1'\sigma_2'}_{m_1m_2} \mathcal{D}_{deph} \rangle &= \frac{\gamma}{2} \sum_i \langle [n_i, [C^{\sigma_1\sigma_2}_{n_1n_2} A^{\sigma_1'\sigma_2'}_{m_1m_2}, n_i]] \rangle \\
&= \frac{\gamma}{2} \sum_i (\langle [n_i, C^{\sigma_1\sigma_2}_{n_1n_2} [A^{\sigma_1'\sigma_2'}_{m_1m_2}, n_i]] \rangle + \langle [n_i, [C^{\sigma_1\sigma_2}_{n_1n_2}, n_i] A^{\sigma_1'\sigma_2'}_{m_1m_2}] \rangle) \\
&= \frac{\gamma}{2} \sum_i \langle (\delta_{im_1} + \delta_{im_2} - \delta_{in_1} - \delta_{in_2}) [n_i, C^{\sigma_1\sigma_2}_{n_1n_2} A^{\sigma_1'\sigma_2'}_{m_1m_2}] \rangle \\
&= -\frac{\gamma}{2} \sum_i (\delta_{im_1} + \delta_{im_2} - \delta_{in_1} - \delta_{in_2})^2 Q^{\sigma_1\sigma_2\sigma_1'\sigma_2'}_{n_1n_2m_1m_2} \\
&= -\gamma (2 + \delta_{n_1n_2} + \delta_{m_1m_2} - \delta_{n_1m_1} \\
&\quad - \delta_{n_1m_2} - \delta_{n_2m_1} - \delta_{n_2m_2}) Q^{\sigma_1\sigma_2\sigma_1'\sigma_2'}_{n_1n_2m_1m_2}
\end{aligned} \tag{B.20}$$

Adding all terms, Equation (4.7) is obtained. Similar calculations for sixth order correlation functions will result Equation (4.8) when higher than sixth order terms are ignored.

Bibliography

1. Dwiputra, D.; Zen, F. P. *Phys. Rev. A* **2021**, *104*, 022205.
2. Engel, G. S.; Calhoun, T. R.; Read, E. L.; Ahn, T.-K.; Mančal, T.; Cheng, Y.-C.; Blankenship, R. E.; Fleming, G. R. *Nature* **2007**, *446*, 782–786.
3. Kassal, I.; Aspuru-Guzik, A. *New Journal of Physics* **2012**, *14*, 053041.
4. León-Montiel, R. d.; Quiroz-Juárez, M. A.; Quintero-Torres, R.; Domínguez-Juárez, J. L.; Moya-Cessa, H. M.; Torres, J. P.; Aragón, J. L. *Scientific Reports* **2015**, *5*, DOI: 10.1038/srep17339.
5. Maier, C.; Brydges, T.; Jurcevic, P.; Trautmann, N.; Hempel, C.; Lanyon, B. P.; Hauke, P.; Blatt, R.; Roos, C. F. *Phys. Rev. Lett.* **2019**, *122*, 050501.
6. Mohseni, M.; Rebentrost, P.; Lloyd, S.; Aspuru-Guzik, A. *The Journal of Chemical Physics* **2008**, *129*, DOI: 10.1063/1.3002335.
7. Viciani, S.; Gherardini, S.; Lima, M.; Bellini, M.; Caruso, F. *Scientific Reports* **2016**, *6*, DOI: 10.1038/srep37791.
8. Zerah-Harush, E.; Dubi, Y. *The Journal of Physical Chemistry Letters* **2018**, *9*, PMID: 29537848, 1689–1695.
9. Zerah-Harush, E.; Dubi, Y. *Physical Review Research* **2020**, *2*, DOI: 10.1103/PhysRevResearch.2.023294.
10. Rebentrost, P.; Mohseni, M.; Kassal, I.; Lloyd, S.; Aspuru-Guzik, A. *New Journal of Physics* **2009**, *11*, 033003.
11. Bloch, I.; Dalibard, J.; Zwerger, W. *Rev. Mod. Phys.* **2008**, *80*, 885–964.
12. D'Errico, C.; Moratti, M.; Lucioni, E.; Tanzi, L.; Deissler, B.; Inguscio, M.; Modugno, G.; Plenio, M. B.; Caruso, F. *New Journal of Physics* **2013**, *15*, 045007.
13. Hess, C. *Physics Reports* **2019**, *811*, Heat transport of cuprate-based low-dimensional quantum magnets with strong exchange coupling, 1–38.
14. Schneider, U.; Hackermüller, L.; Ronzheimer, J. P.; Will, S.; Braun, S.; Best, T.; Bloch, I.; Demler, E.; Mandt, S.; Rasch, D.; et al. *Nature Physics* **2012**, *8*, 213–218.
15. Sologubenko, A. V.; Giannó, K.; Ott, H. R.; Ammerahl, U.; Revcolevschi, A. *Phys. Rev. Lett.* **2000**, *84*, 2714–2717.
16. Sologubenko, A. V.; Lorenz, T.; Ott, H. R.; Freimuth, A. *Journal of Low Temperature Physics* **2007**, *147*, 387–403.

17. Landi, G. T.; Poletti, D.; Schaller, G. *Rev. Mod. Phys.* **2022**, *94*, 045006.

18. Bertini, B.; Heidrich-Meisner, F.; Karrasch, C.; Prosen, T.; Steinigeweg, R.; Žnidari č, M. *Rev. Mod. Phys.* **2021**, *93*, 025003.

19. Lindblad, G. *Communications in Mathematical Physics* **1976**, *48*, 119–130.

20. Breuer, H.-P.; Petruccione, F., *The theory of Open Quantum Systems*; Clarendon: 2010.

21. Santos, J. P.; Landi, G. T. *Physical Review E* **2016**, *94*, DOI: 10.1103/physreve.94.062143.

22. Nakajima, S. *Progress of Theoretical Physics* **1958**, *20*, 948–959.

23. Misra, B.; Sudarshan, E. C. G. *Journal of Mathematical Physics* **1977**, *18*, 756–763.

24. Hubbard, J. *Proceedings of the Royal Society of London. Series A, Mathematical and Physical Sciences* **1963**, *276*, 238–257.

25. Benenti, G.; Casati, G.; Prosen, T. ž.; Rossini, D.; Žnidari č, M. *Phys. Rev. B* **2009**, *80*, 035110.

26. Karevski, D.; Platini, T. *Phys. Rev. Lett.* **2009**, *102*, 207207.

27. Mendoza-Arenas, J. J.; Grujic, T.; Jaksch, D.; Clark, S. R. *Phys. Rev. B* **2013**, *87*, 235130.